

**Electronic Supporting Information**

**Functionalization of 10-azacorroles: nitration, bromination and acylation**

Sha Li, Yuhuan Zhu, Xiaofang Li,\* Shaowei Zhang,\* Michał J. Białek, and Piotr J. Chmielewski\*

Key Laboratory of Theoretical Organic Chemistry and Functional Molecules, Ministry of Education,  
School of Chemistry and Chemical Engineering, Hunan University of Science and Technology,  
Xiangtan, Hunan 411201, China

E-mail: [lixiaofang@iccas.ac.cn](mailto:lixiaofang@iccas.ac.cn), [swzhang@hnust.edu.cn](mailto:swzhang@hnust.edu.cn), [piotr.chmielewski@uwr.edu.pl](mailto:piotr.chmielewski@uwr.edu.pl)

## Table of contents

- Figs. S1-S2** NMR spectra of **2a**.  
**Figs. S3-S4** NMR spectra of **2b**.  
**Figs. S5-S6** NMR spectra of **3a**.  
**Figs. S7-S8** NMR spectra of **3b**.  
**Figs. S9-S10** NMR spectra of **4a**.  
**Figs. S11-S12** NMR spectra of **4b**.  
**Figs. S13-S18** NMR spectra of **5a**.  
**Figs. S19-S20** NMR spectra of **5b**.  
**Figs. S21-S22** NMR spectra of **5c**.  
**Figs. S23-S24** NMR spectra of **5d**.  
**Fig. S25** HRMS spectrum of **2a**.  
**Fig. S26** HRMS spectrum of **2b**.  
**Fig. S27** HRMS spectrum of **3a**.  
**Fig. S28** HRMS spectrum of **3b**.  
**Fig. S29** HRMS spectrum of **4a**.  
**Fig. S30** HRMS spectrum of **4b**.  
**Fig. S31** HRMS spectrum of **5a**.  
**Fig. S32** HRMS spectrum of **5b**.  
**Fig. S33** HRMS spectrum of **5c**.  
**Fig. S34** HRMS spectrum of **5d**.  
**Fig. S35** UV-vis spectrum of **2a**.  
**Fig. S36**. UV-vis spectrum of **2b**.  
**Fig. S37**. UV-vis spectrum of **3a**.  
**Fig. S38**. UV-vis spectrum of **3b**.  
**Fig. S39**. UV-vis spectrum of **4a**.  
**Fig. S40**. UV-vis spectrum of **4b**.  
**Fig. S41**. UV-vis spectrum of **5a**.  
**Fig. S42** UV-vis spectrum of **5b**.  
**Fig. S43**. UV-vis spectrum of **5c**.  
**Fig. S44**. UV-vis spectrum of **5d**.  
**Fig. S45**. Kohn-Sham frontier orbital distributions in **1a**.  
**Fig. S46**. Electrostatic potential and charge distribution in **1a** calculated by NBO approach.  
**Fig. S47**. Calculated and experimental UV-Vis spectra for **1a-5a**.  
**Fig. S48**. Cyclic and differential pulse voltammograms for **2a**.  
**Fig. S49**. Cyclic and differential pulse voltammograms for **2b**.  
**Fig. S50**. Cyclic and differential pulse voltammograms for **3a**.  
**Fig. S51**. Cyclic and differential pulse voltammograms for **3b**.  
**Fig. S52**. Cyclic and differential pulse voltammograms for **4a**.  
**Fig. S53**. Cyclic and differential pulse voltammograms for **4b**.  
**Fig. S54**. Cyclic and differential pulse voltammograms for **5a**.  
**Fig. S55**. Cyclic and differential pulse voltammograms for **5b**.  
**Fig. S56**. Cyclic and differential pulse voltammograms for **5c**.  
**Fig. S57**. Cyclic and differential pulse voltammograms for **5d**.  
**Table S1**. Electrochemical data for the 10-azacorrole derivatives.  
**Table S2**. Electronic transitions calculated for **1a**.  
**Table S3**. Electronic transitions calculated for **2a**.  
**Table S4**. Electronic transitions calculated for **3a**.  
**Table S5**. Electronic transitions calculated for **4a**.  
**Table S6**. Electronic transitions calculated for **5a**.  
**Fig. S56**. Correlations of calculated HOMO energy with the first oxidation potentials for the compounds **1a-5a**.  
**Fig. S57**. Correlations of calculated LUMO energy with the first reduction potentials for the compounds **1a-5a**.  
**Table S7**. Computational details for the optimized structures of compounds.  
**Figure S58** DFT optimized models and relative energies of possible cationic intermediates

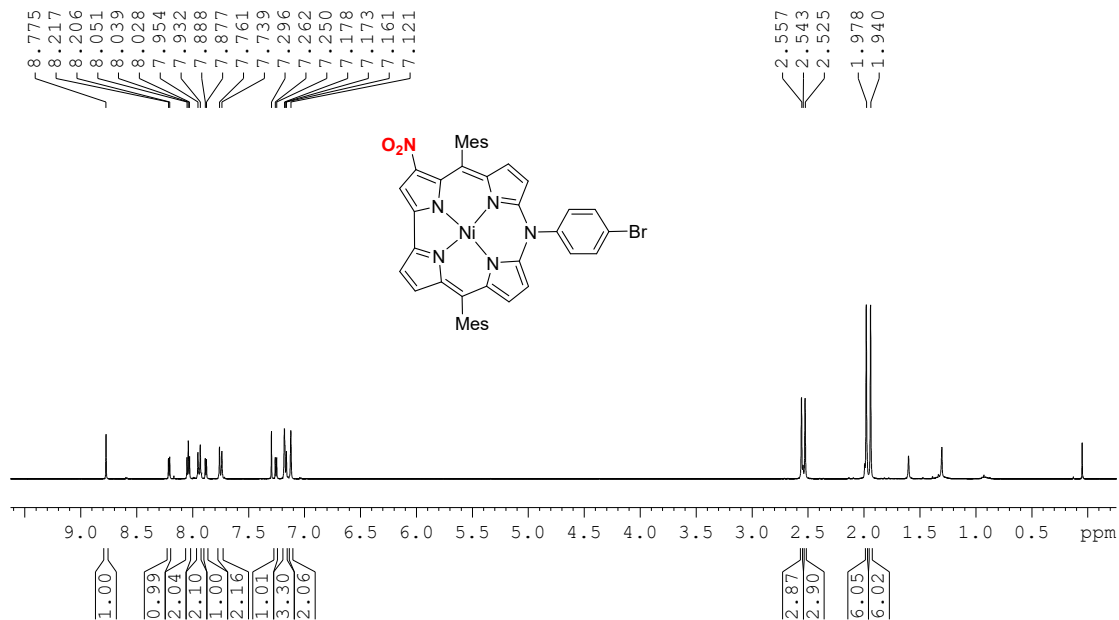


Figure S1. <sup>1</sup>H NMR spectrum of 2a (400 MHz, 298 K, CDCl<sub>3</sub>).

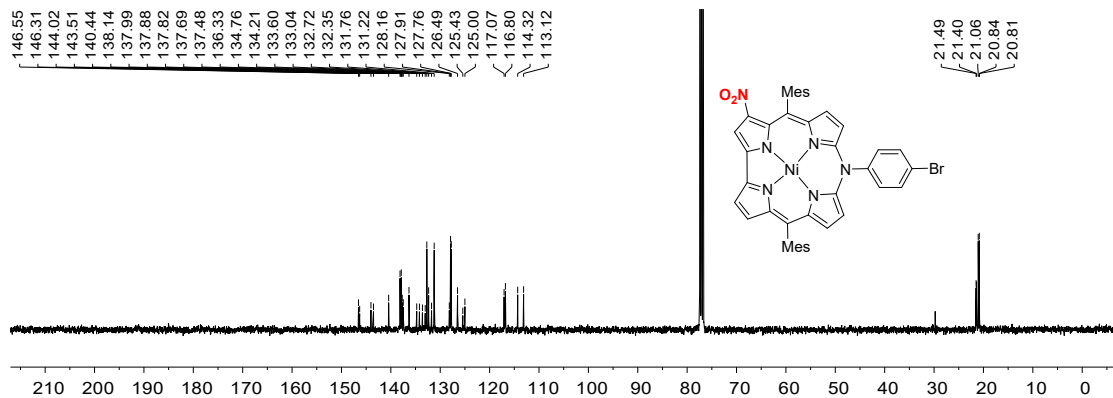
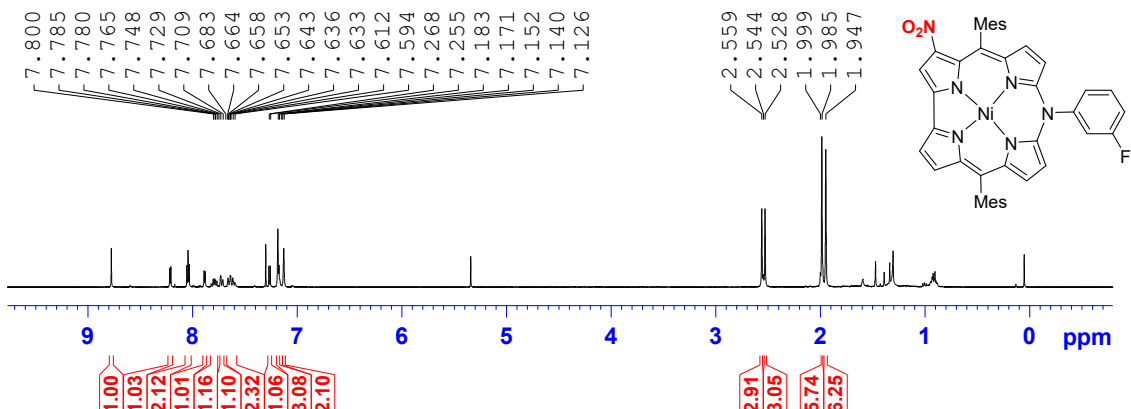
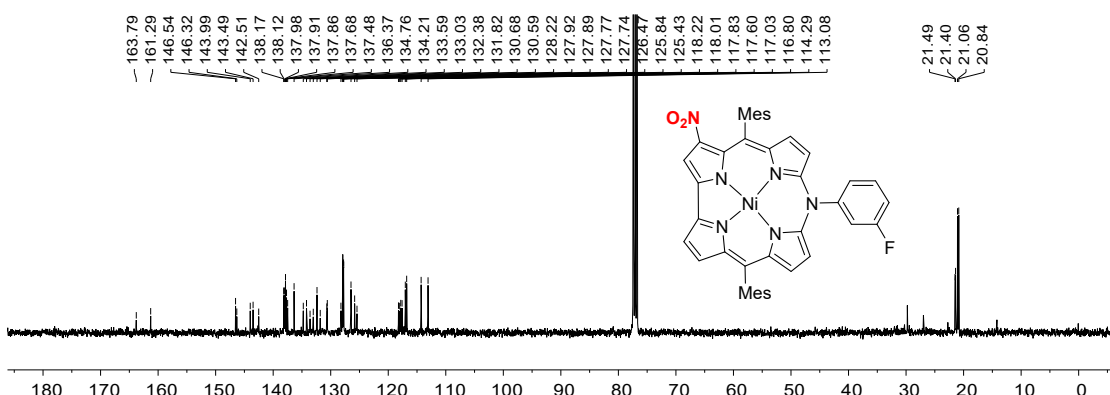


Figure S2. <sup>13</sup>C NMR spectrum of 2a (100 MHz, 298 K, CDCl<sub>3</sub>).



**Figure S3.**  $^1\text{H}$  NMR spectrum of **2b** (400 MHz, 298 K,  $\text{CDCl}_3$ ).



**Figure S4.**  $^{13}\text{C}$  NMR spectrum of **2b** (100 MHz, 298 K,  $\text{CDCl}_3$ ).

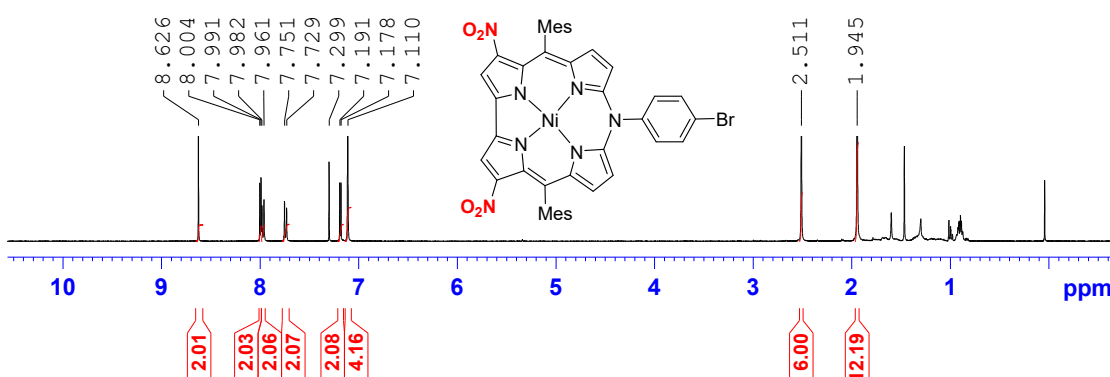


**Figure S5.**  $^1\text{H}$  spectrum of **3a** (400 MHz, 298 K,  $\text{CDCl}_3$ ).

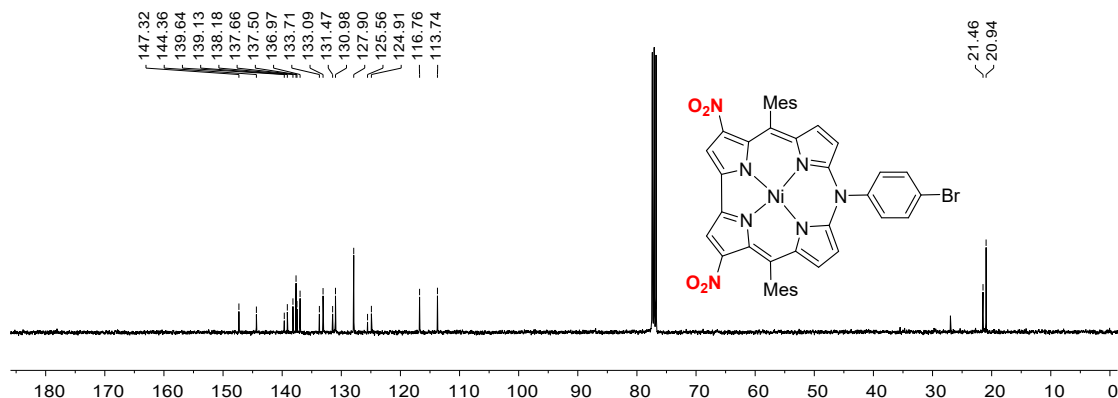


**Figure S6.**  $^{13}\text{C}$  spectrum of **3a** (100 MHz, 298 K,  $\text{CDCl}_3$ ).

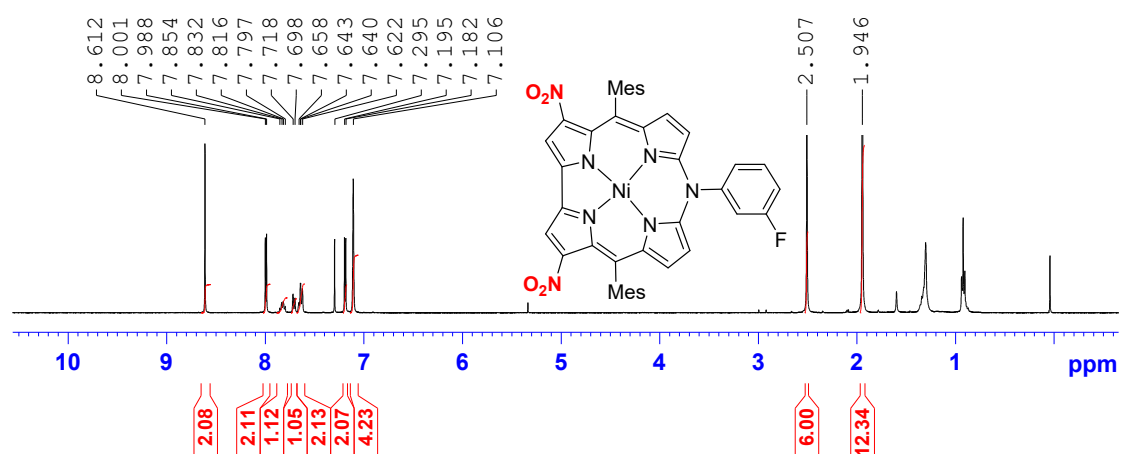


**Figure S7.**  $^1\text{H}$  NMR spectrum of **3b** (400 MHz, 298 K,  $\text{CDCl}_3$ ).

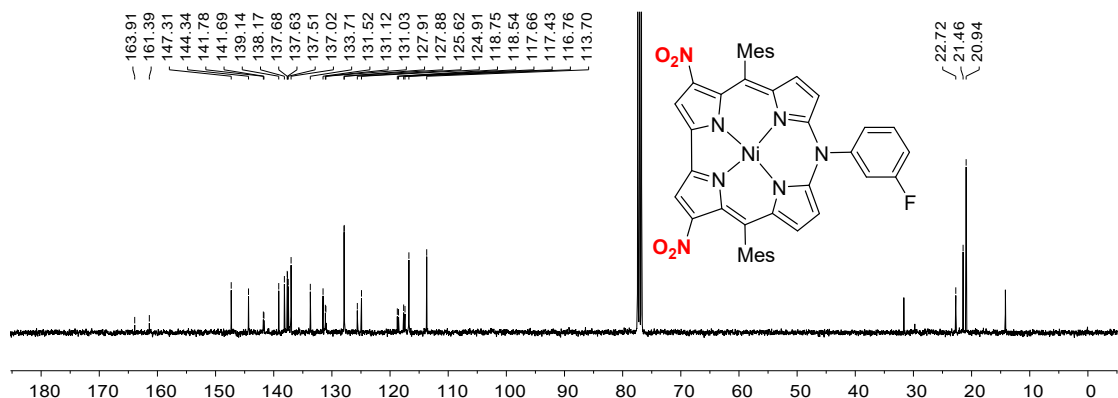


**Figure S8.**  $^{13}\text{C}$  NMR spectrum of **3b** (100 MHz, 298 K,  $\text{CDCl}_3$ ).

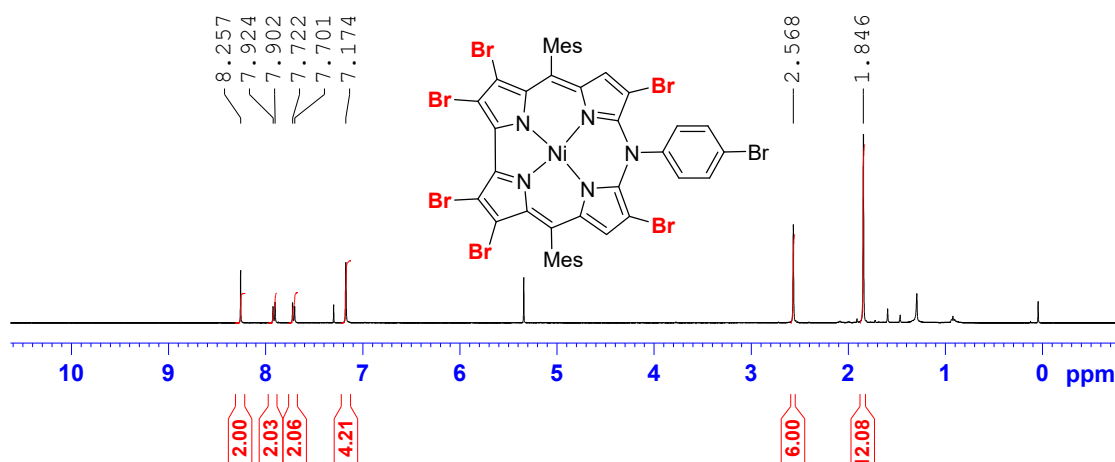


Figure S9. <sup>1</sup>H spectrum of **4a** (400 MHz, 298 K, CDCl<sub>3</sub>).

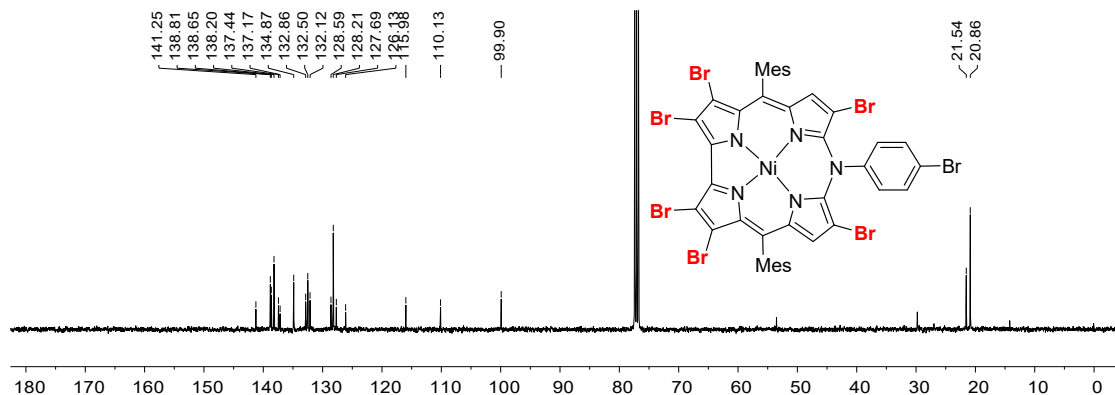


Figure S10. <sup>13</sup>C spectrum of **4a** (100 MHz, 298 K, CDCl<sub>3</sub>).

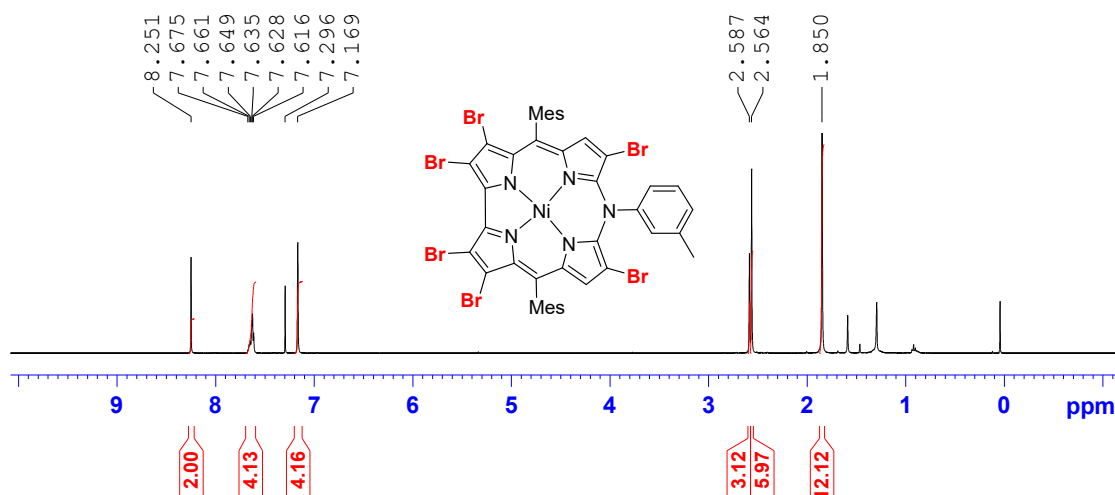


Figure S11. <sup>1</sup>H spectrum of **4b** (400 MHz, 298 K, CDCl<sub>3</sub>).

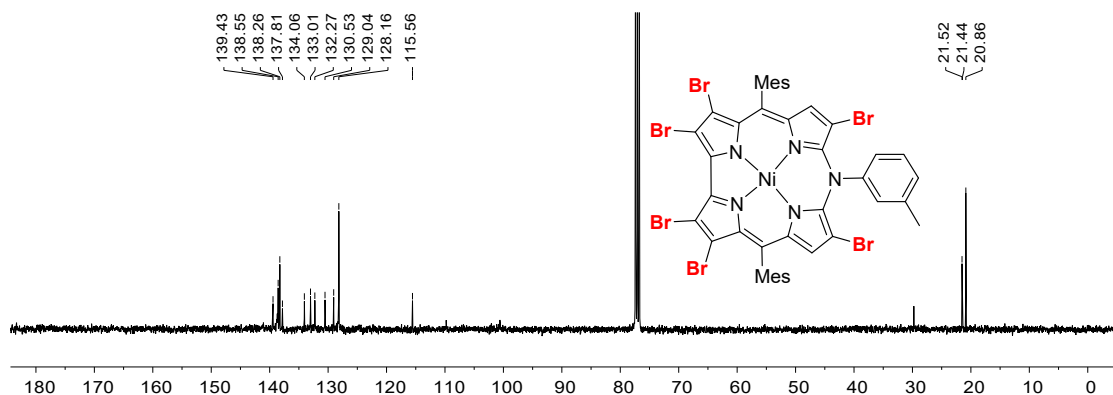


Figure S12. <sup>13</sup>C spectrum of **4b** (100 MHz, 298 K, CDCl<sub>3</sub>).

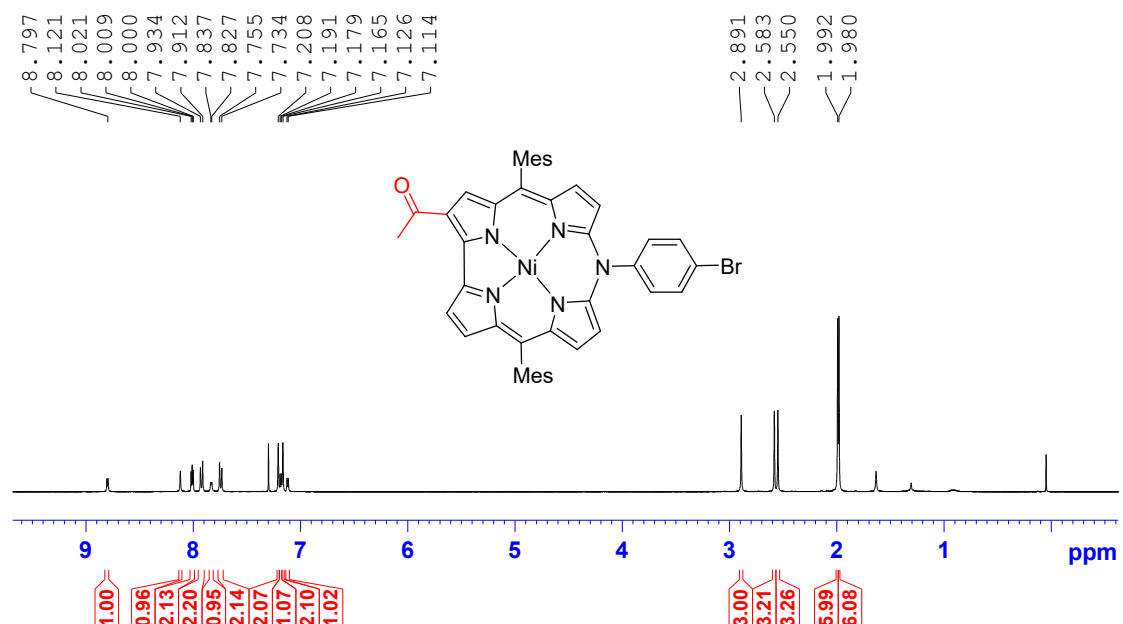
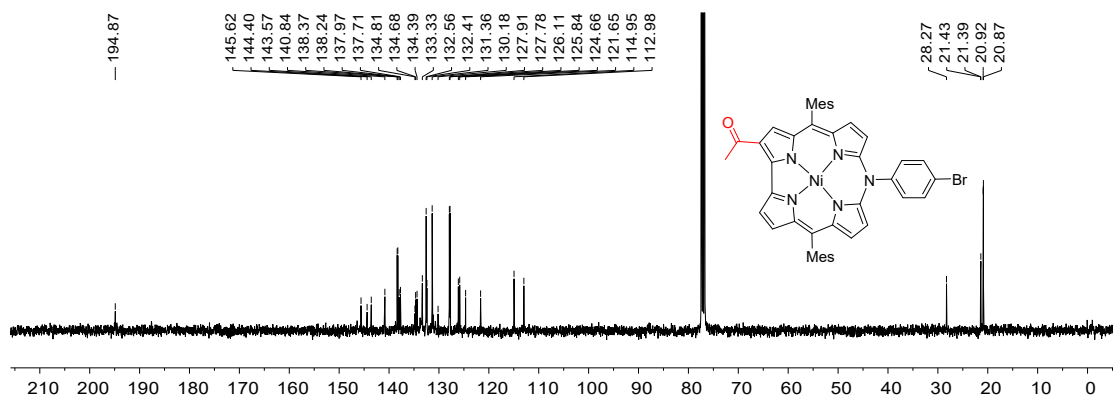
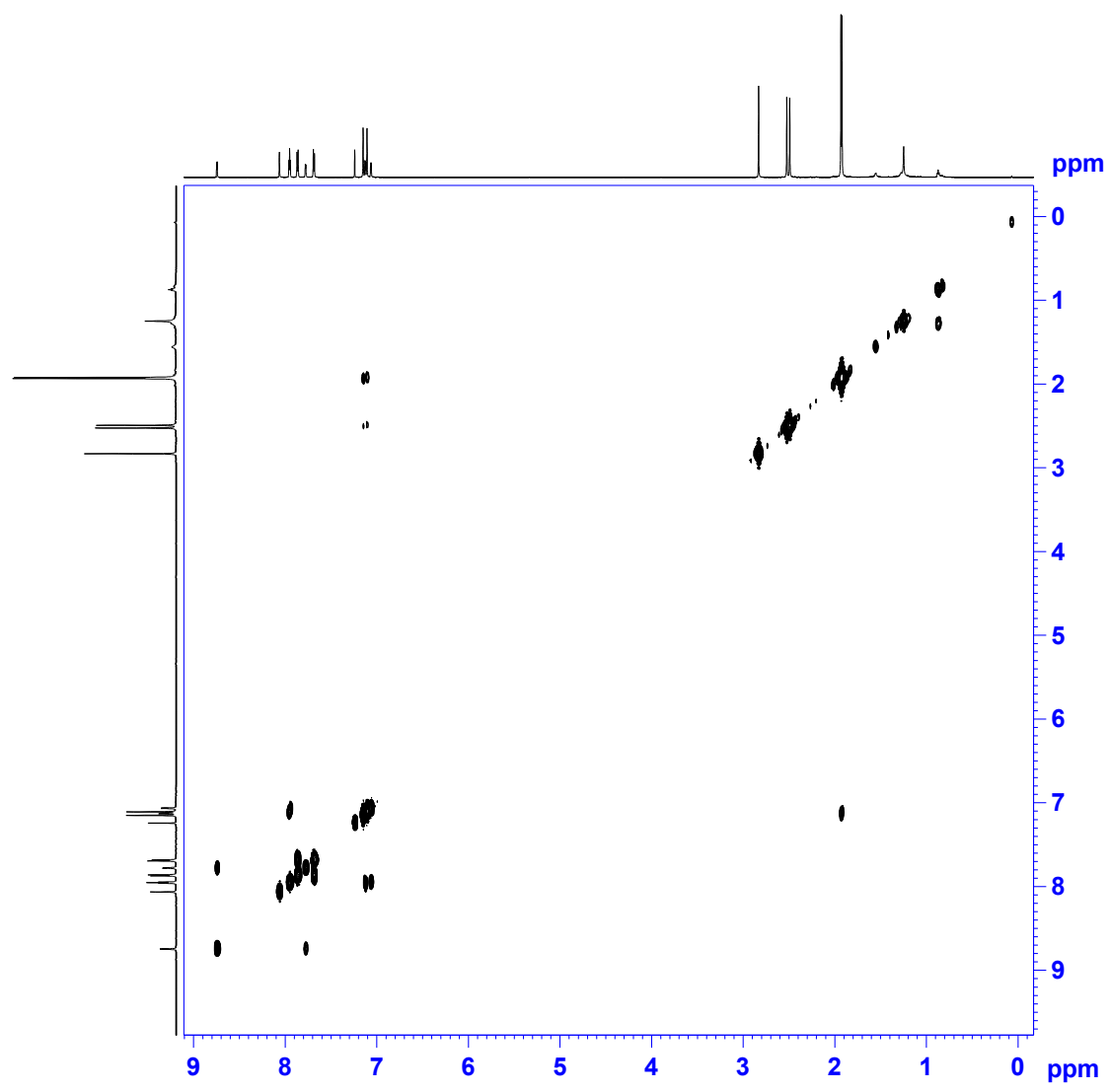


Figure S13. <sup>1</sup>H NMR spectrum of **5a** (400 MHz, 298 K, CDCl<sub>3</sub>).



**Figure S14.** <sup>13</sup>C NMR spectrum of **5a** (100 MHz, 298 K, CDCl<sub>3</sub>).



**Figure S15.** <sup>1</sup>H, <sup>1</sup>H COSY spectrum of **5a** (700 MHz, 298 K, CDCl<sub>3</sub>).

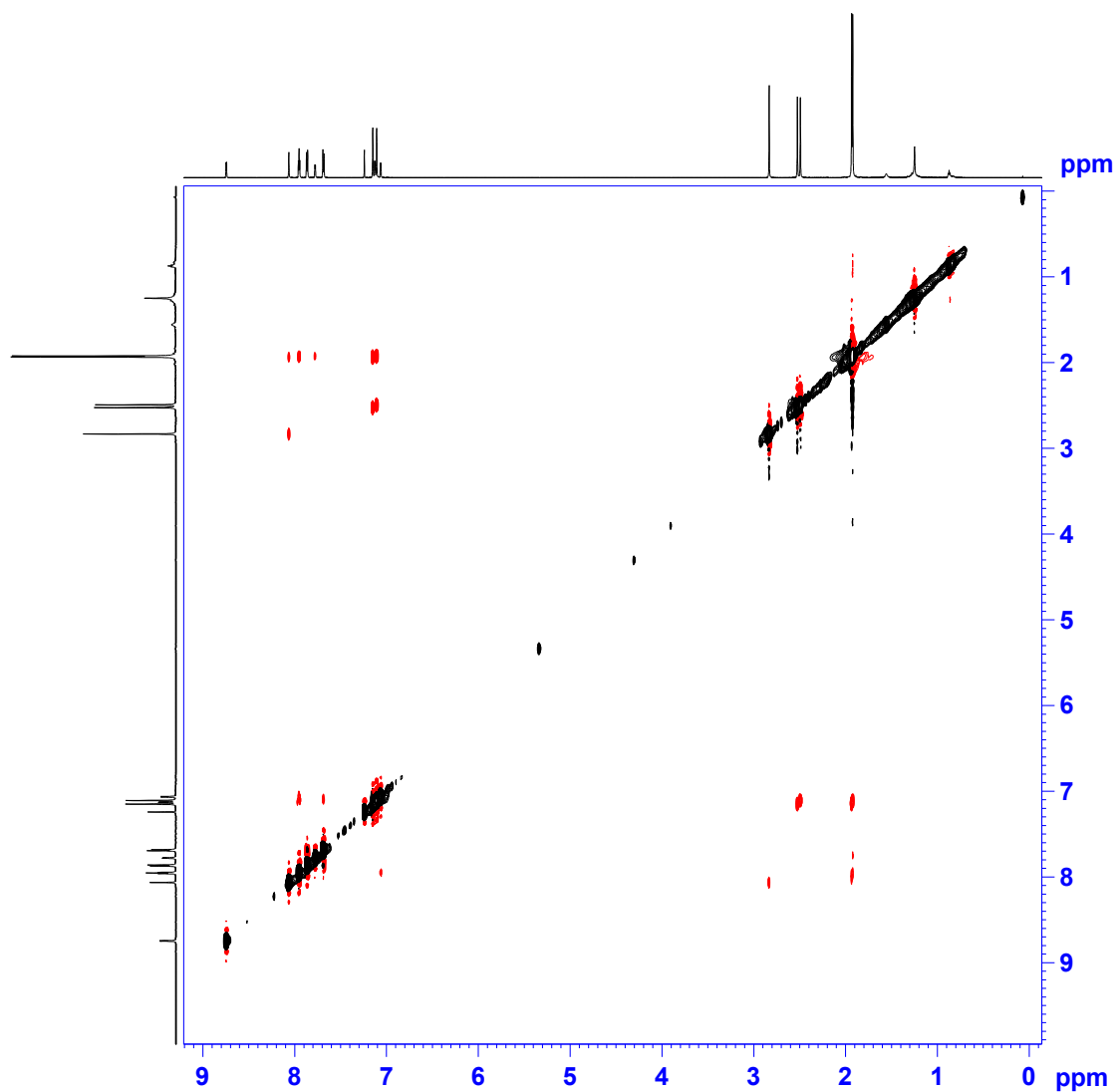


**Figure S16.**  $^1\text{H}$ ,  $^1\text{H}$  NOESY spectrum of **5a** (700 MHz, 298 K,  $\text{CDCl}_3$ ).

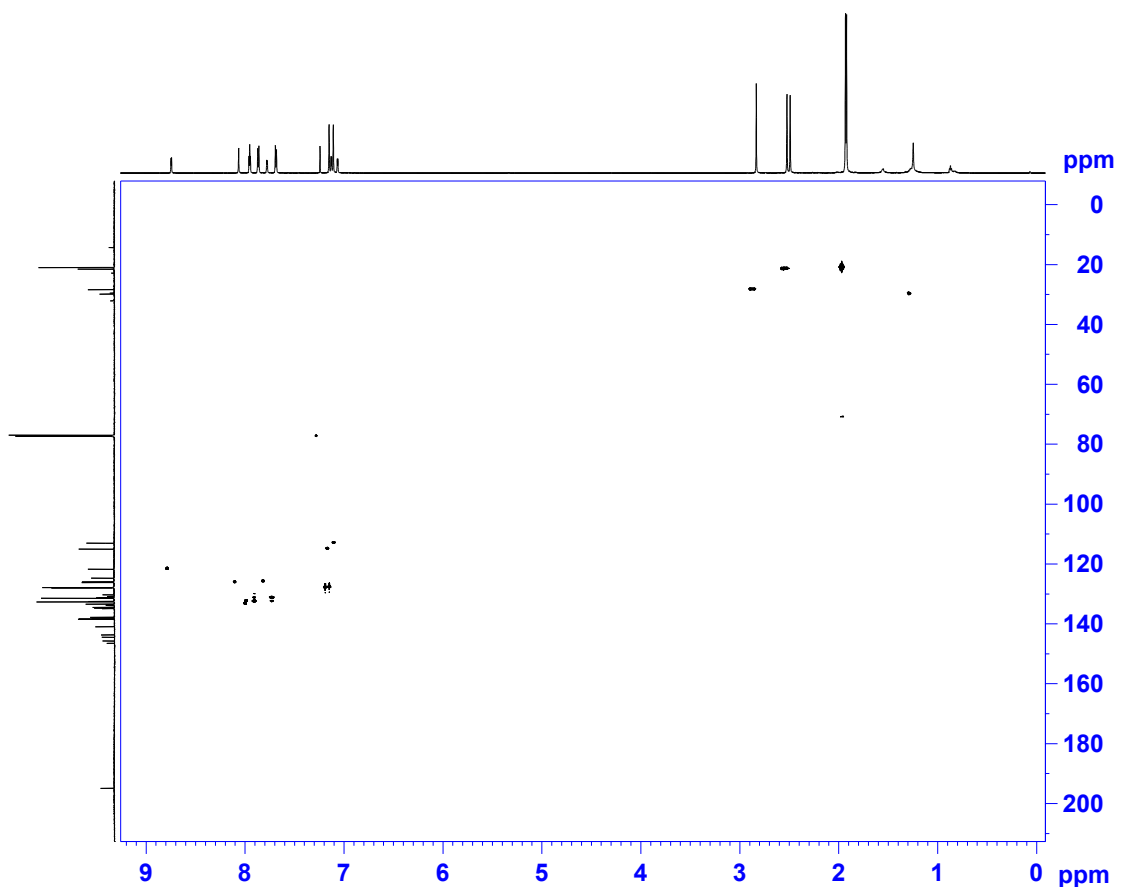


**Figure S17.**  $^1\text{H}$ ,  $^{13}\text{C}$  HSQC spectrum of **5a** (700/175 MHz, 298 K,  $\text{CDCl}_3$ ).

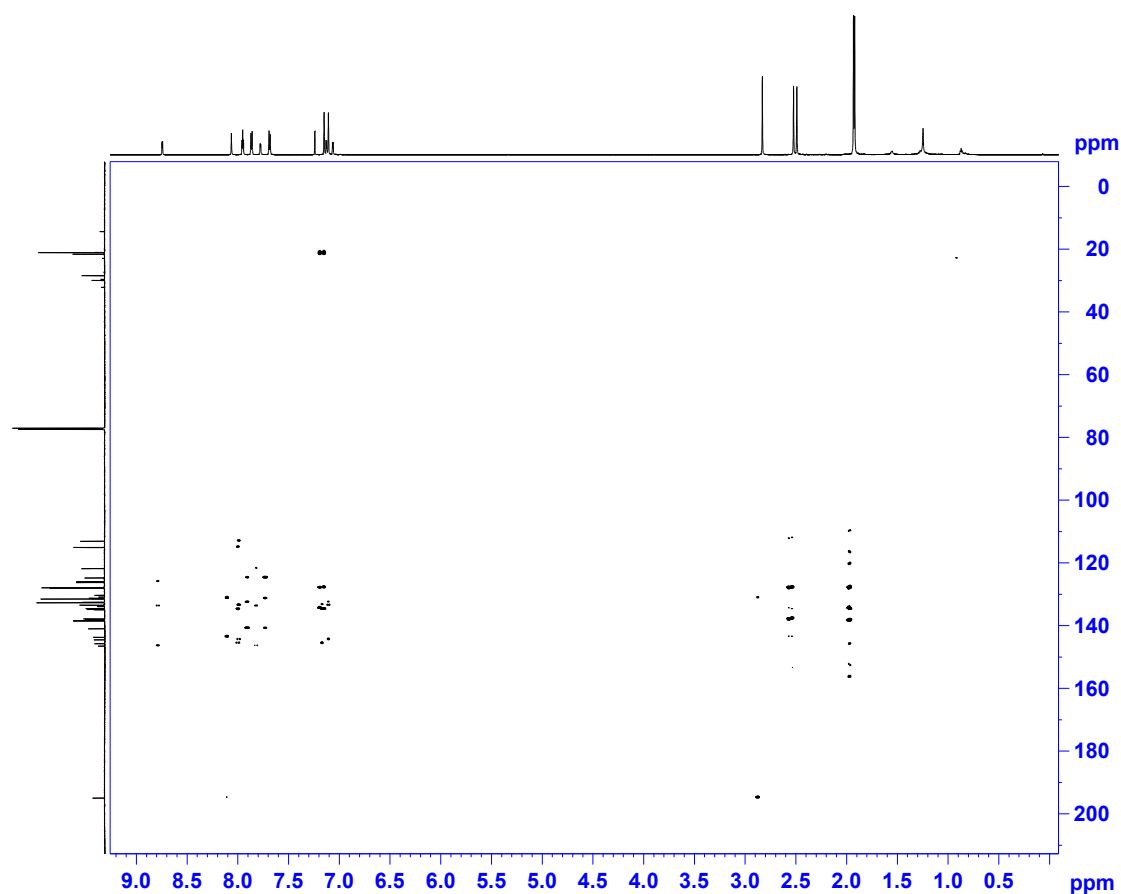


**Figure S18.** <sup>1</sup>H, <sup>13</sup>C HMBC spectrum of **5a** (700/175 MHz, 298 K, CDCl<sub>3</sub>).

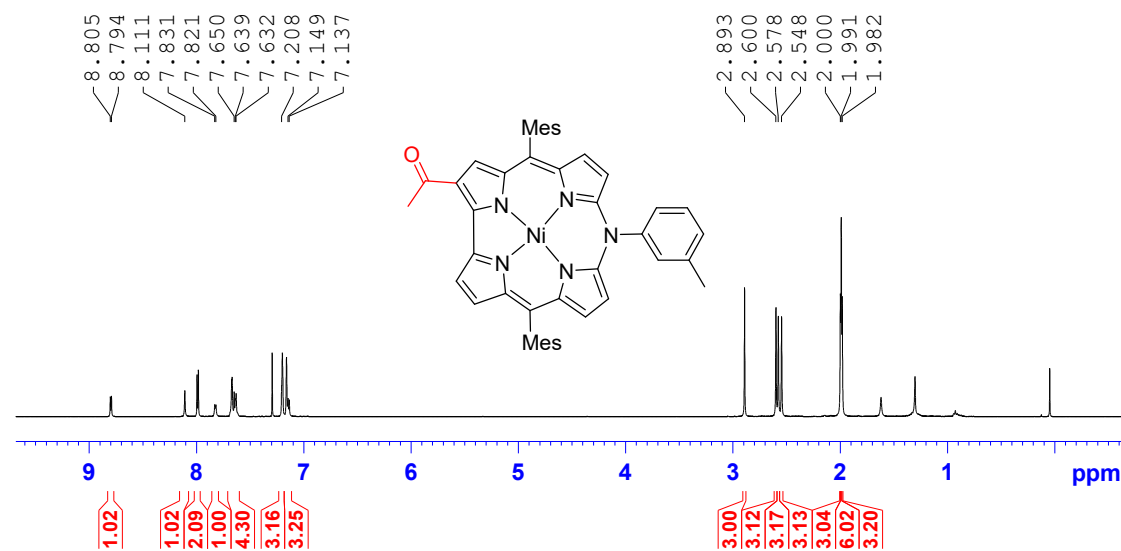


**Figure S19.** <sup>1</sup>H NMR spectrum of **5b** (400 MHz, 298 K, CDCl<sub>3</sub>).

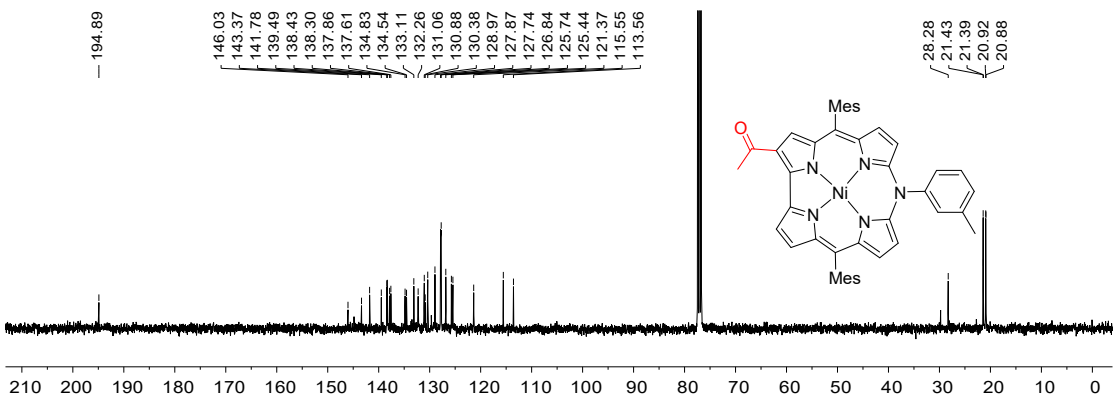


**Figure S20.**  $^{13}\text{C}$  NMR spectrum of **5b** (100 MHz, 298 K,  $\text{CDCl}_3$ ).

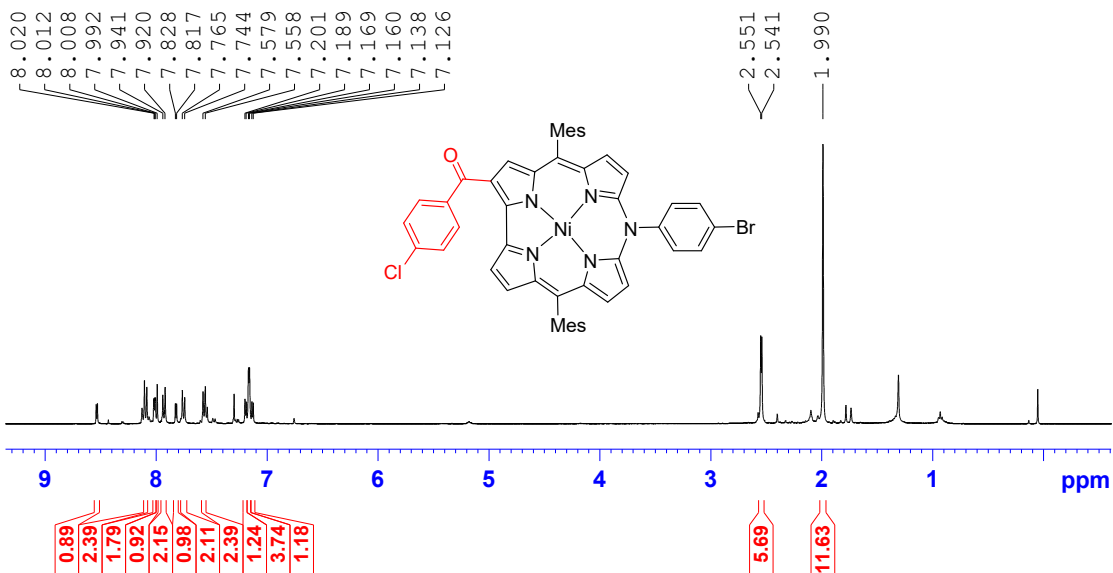


**Figure S21.**  $^1\text{H}$  NMR spectrum of **5c** (400 MHz, 298 K,  $\text{CDCl}_3$ ).

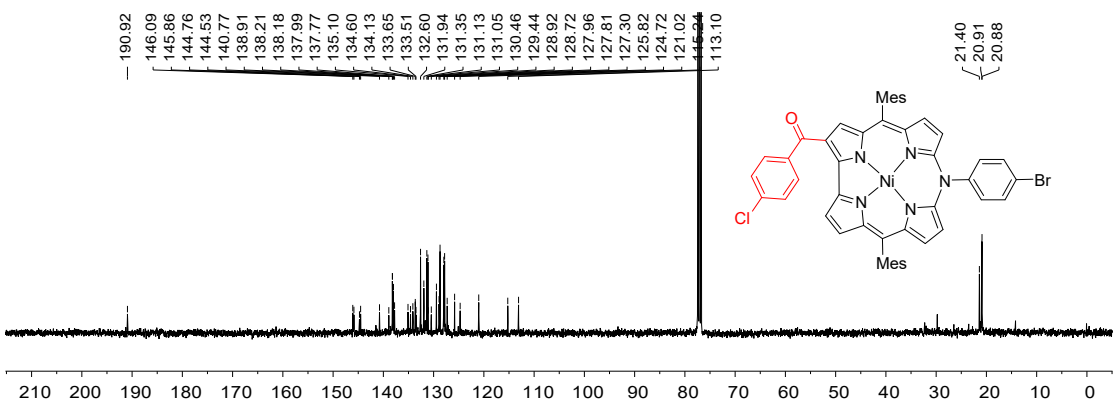


**Figure S22.**  $^{13}\text{C}$  NMR spectrum of **5c** (100 MHz, 298 K,  $\text{CDCl}_3$ ).

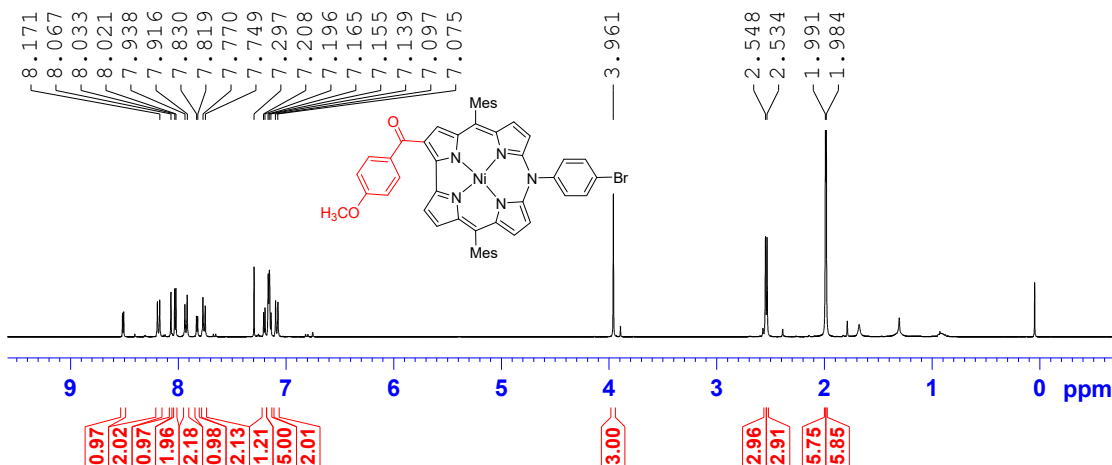


**Figure S23.**  $^1\text{H}$  NMR spectrum of **5d** (400Mhz, 298 K,  $\text{CDCl}_3$ ).

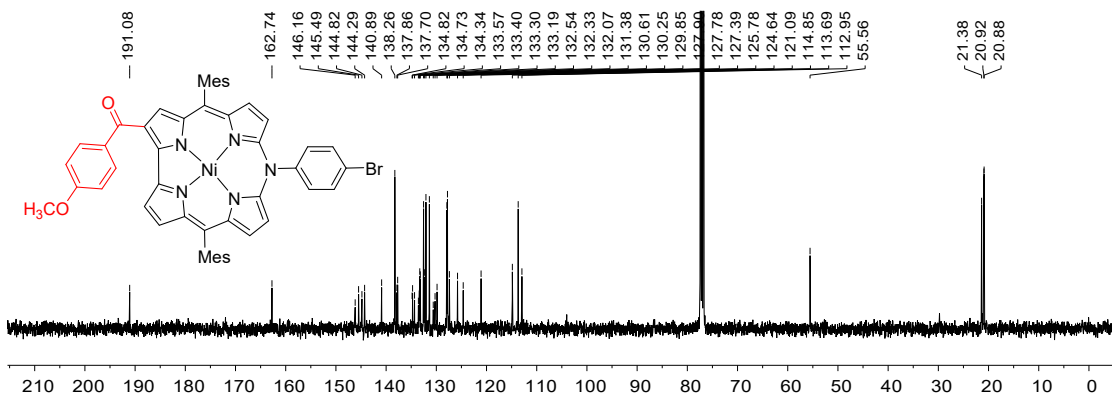


**Figure S24.**  $^{13}\text{C}$  NMR spectrum of **5d** (100 Mhz, 298 K,  $\text{CDCl}_3$ ).

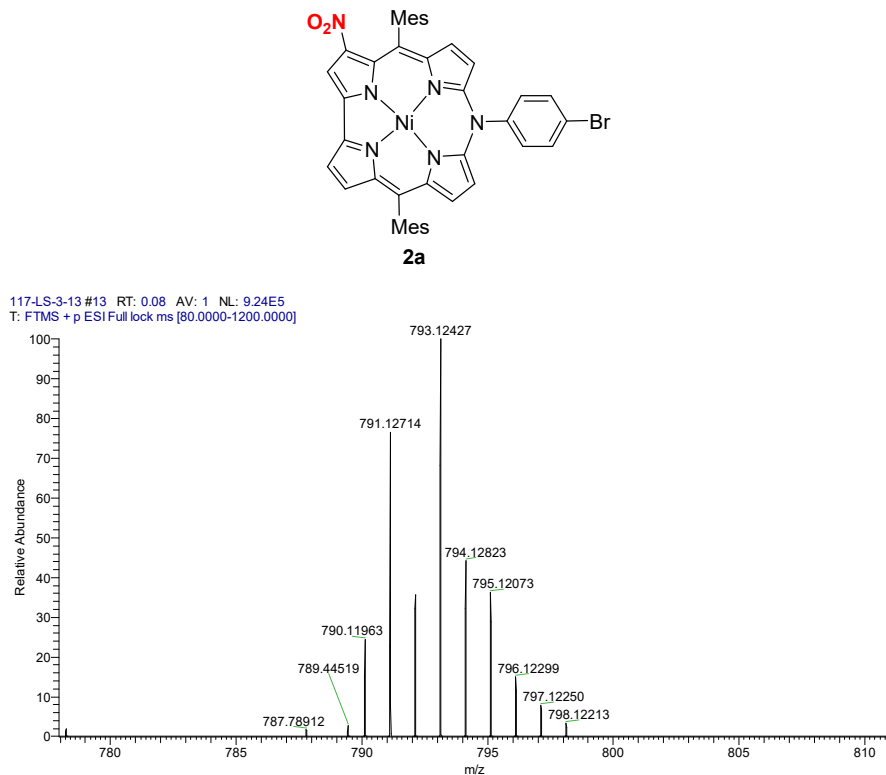


**Figure S25.** ESI(+) HRMS spectrum of **2a**.

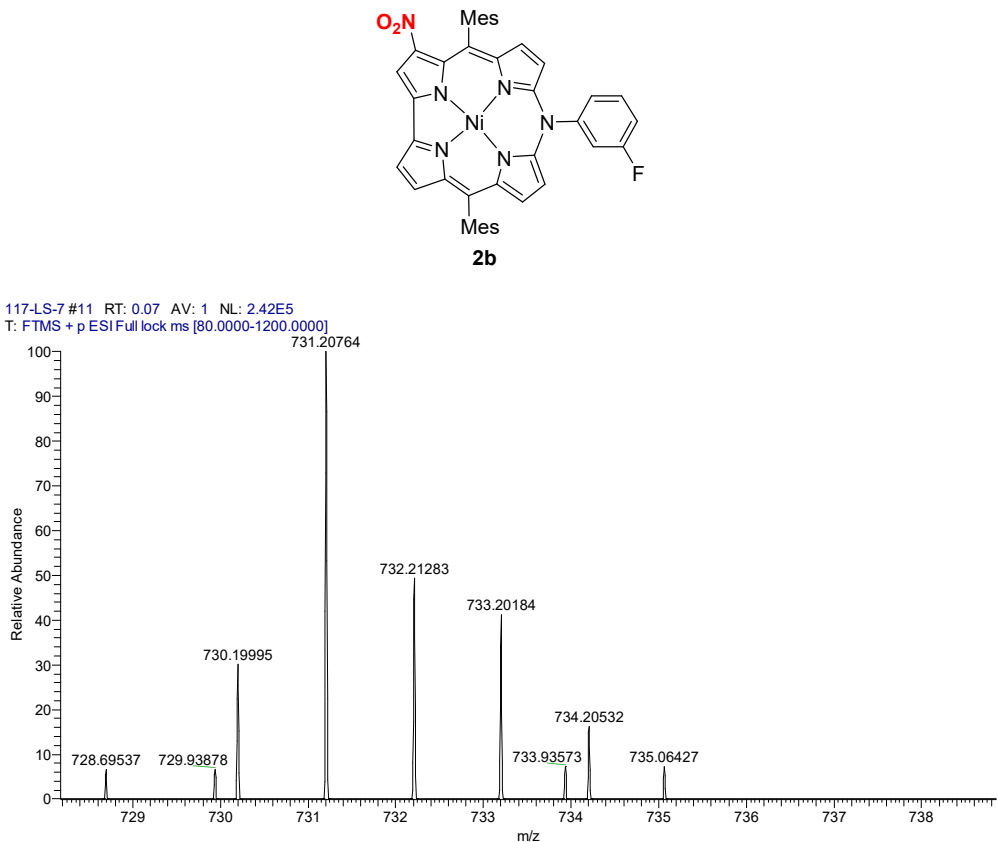


**Figure S26.** ESI(-) HRMS spectrum of **2b**.

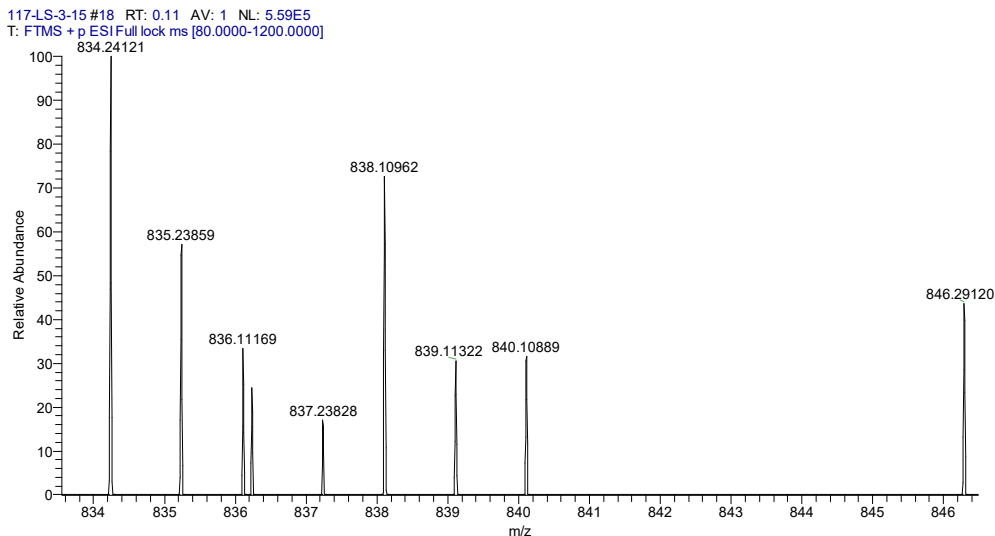
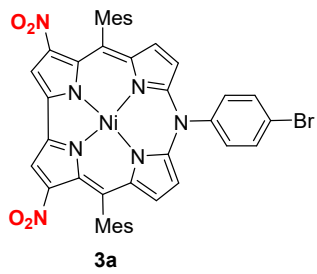


**Figure S27.** ESI(+) HRMS spectrum of **3a**.

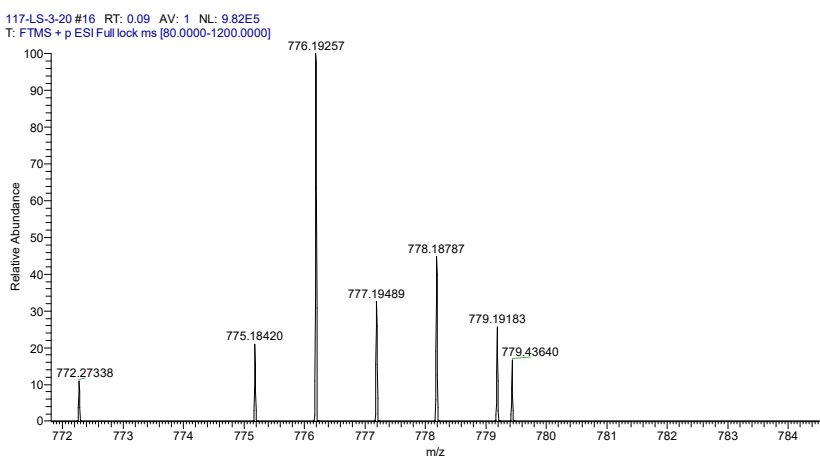
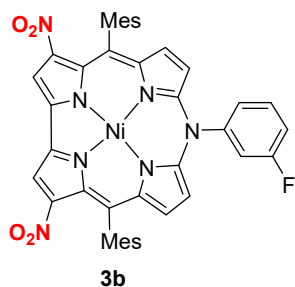


**Figure S28.** ESI(+) HRMS spectrum of **3b**.

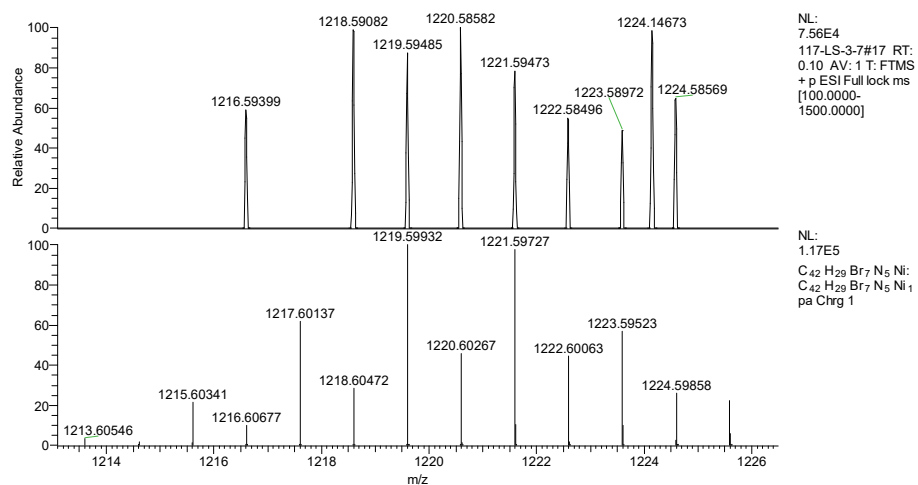
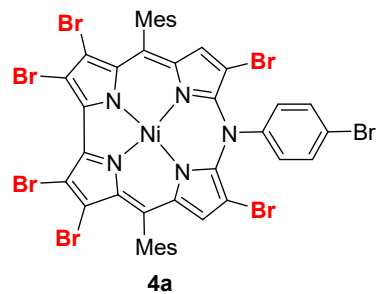


**Figure S29.** ESI(+) HRMS spectrum of **4a**.

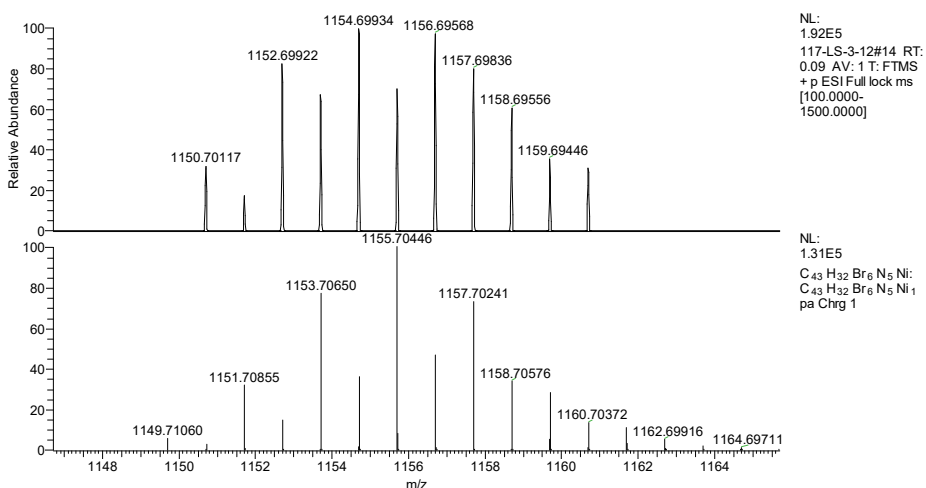
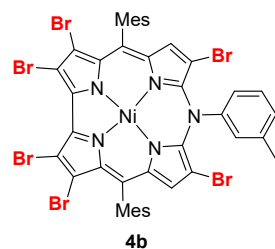


**Figure S30.** ESI(+) HRMS spectrum of **4b**.

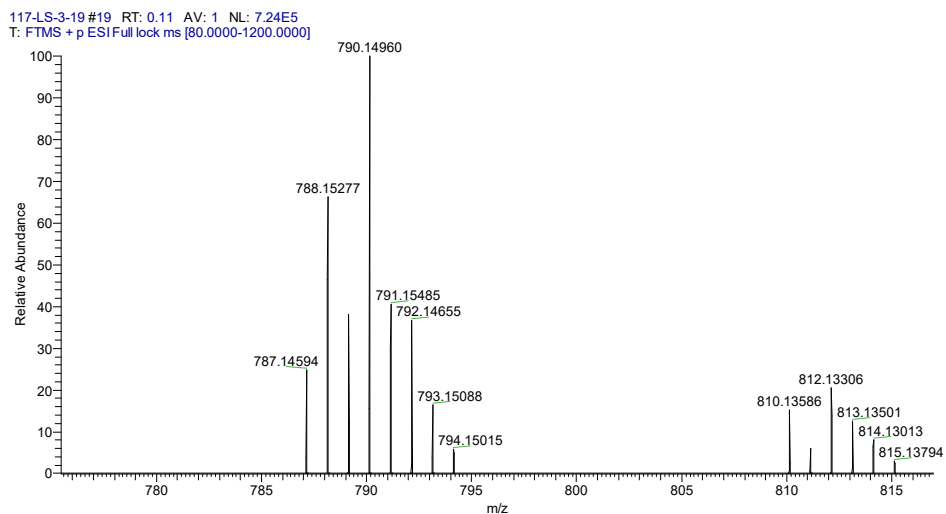
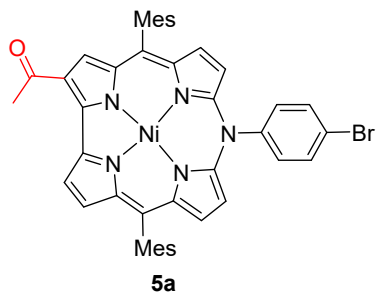


**Figure S31.** ESI(+) HRMS spectrum of **5a**.

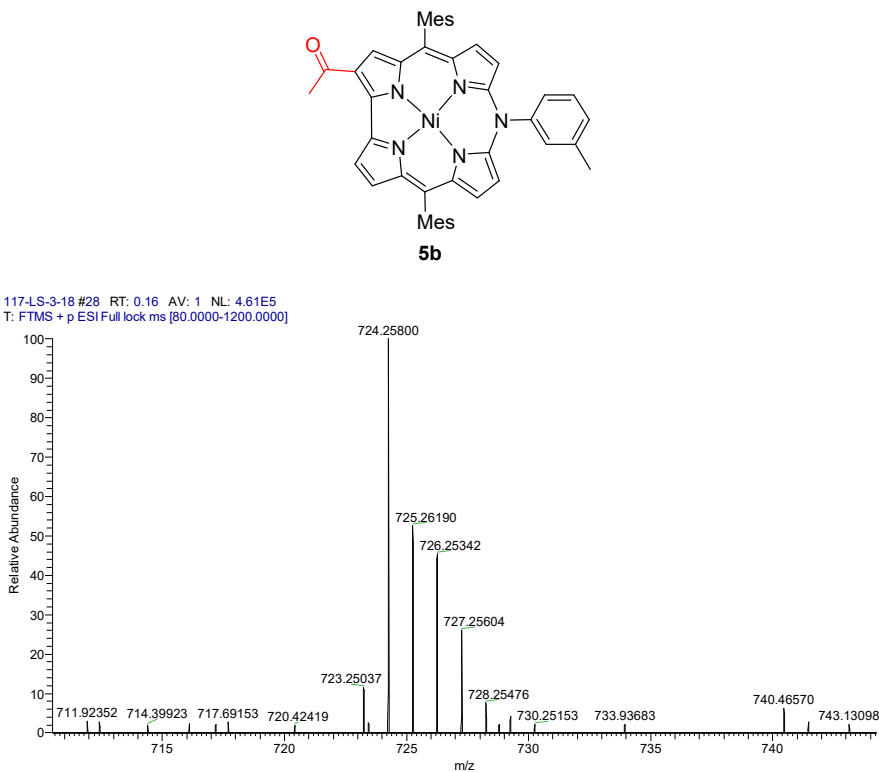


**Figure S32.** ESI(+) HRMS spectrum of **5b**.

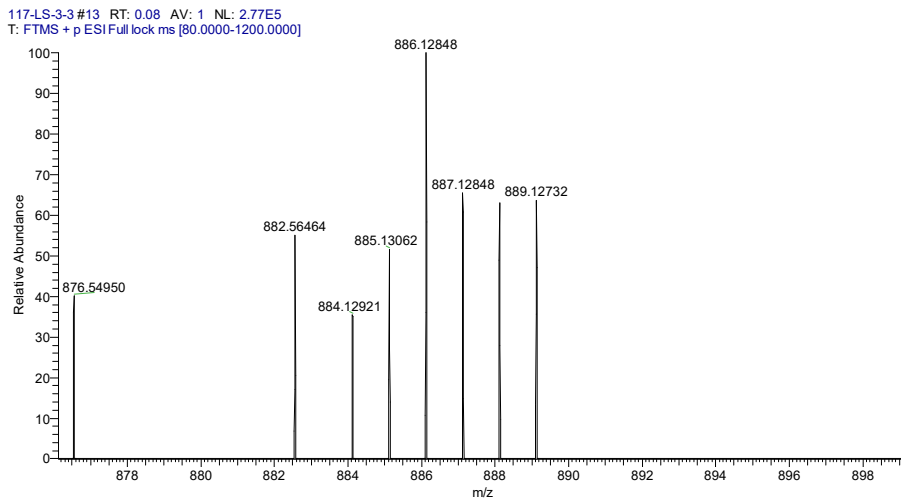
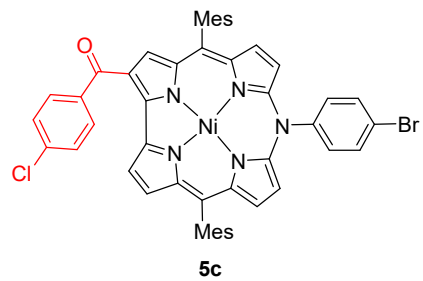


**Figure S33.** ESI(+) HRMS spectrum of **5c**

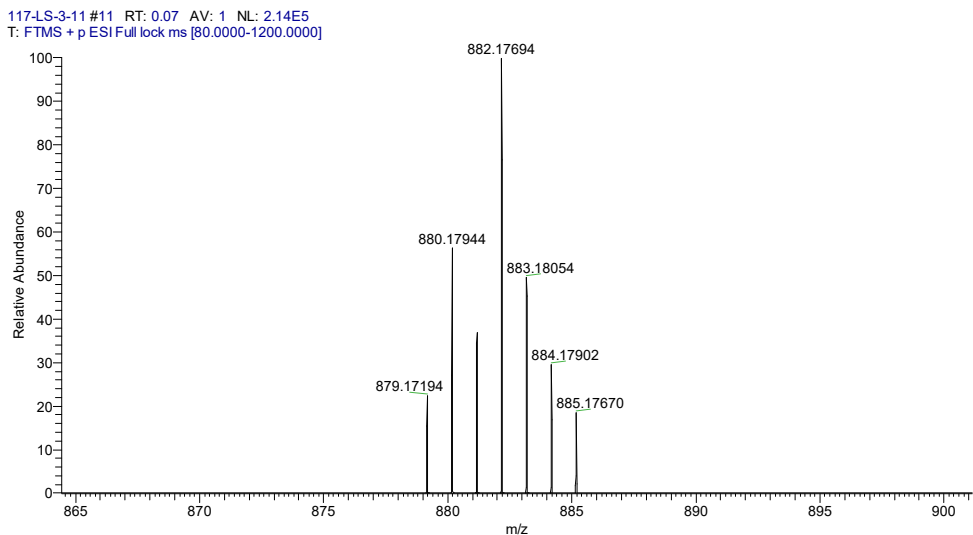
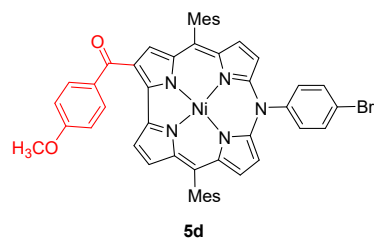


**Figure S34.** ESI(+) HRMS spectrum of **5d**.

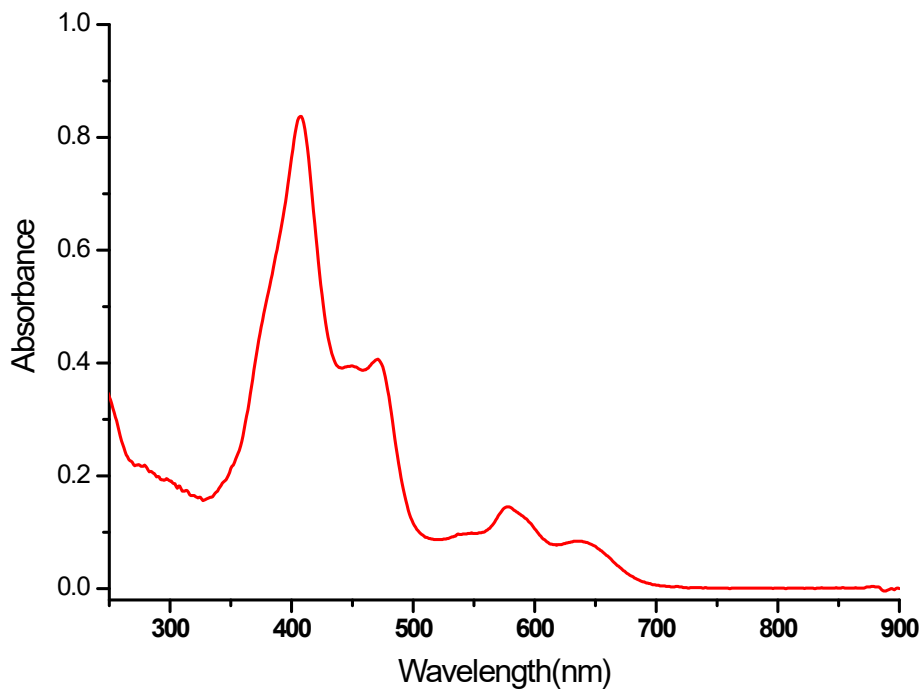


**Figure S35.** UV-vis spectrum of **2a** ( $\text{CH}_2\text{Cl}_2$ ).

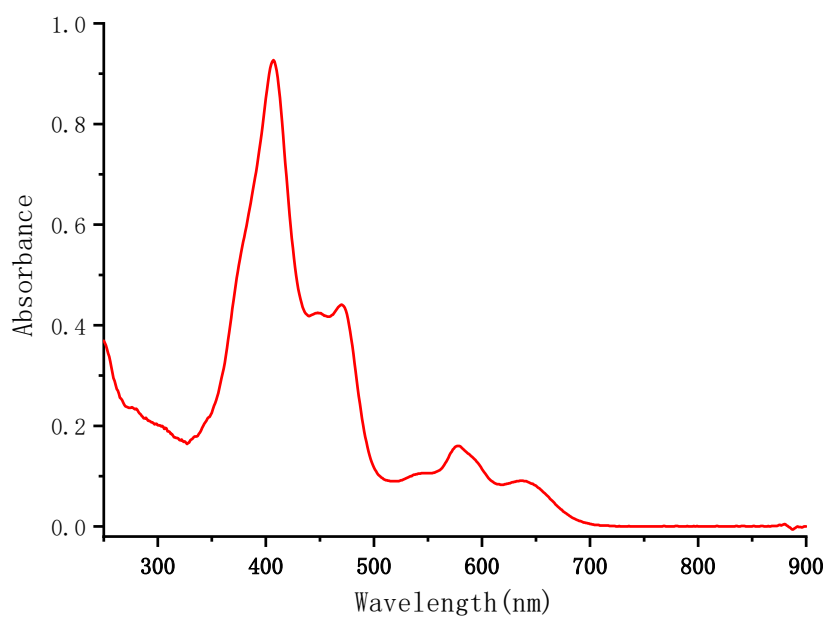


**Figure S36.** UV-vis spectrum of **2b** ( $\text{CH}_2\text{Cl}_2$ ).

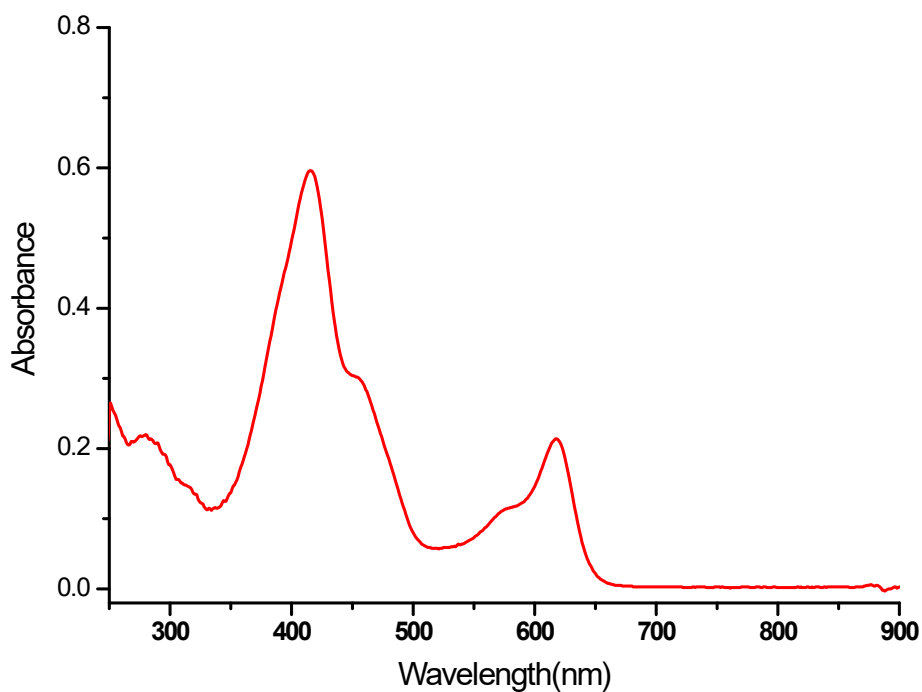


**Figure S37.** UV-vis spectrum of **3a** ( $\text{CH}_2\text{Cl}_2$ ).

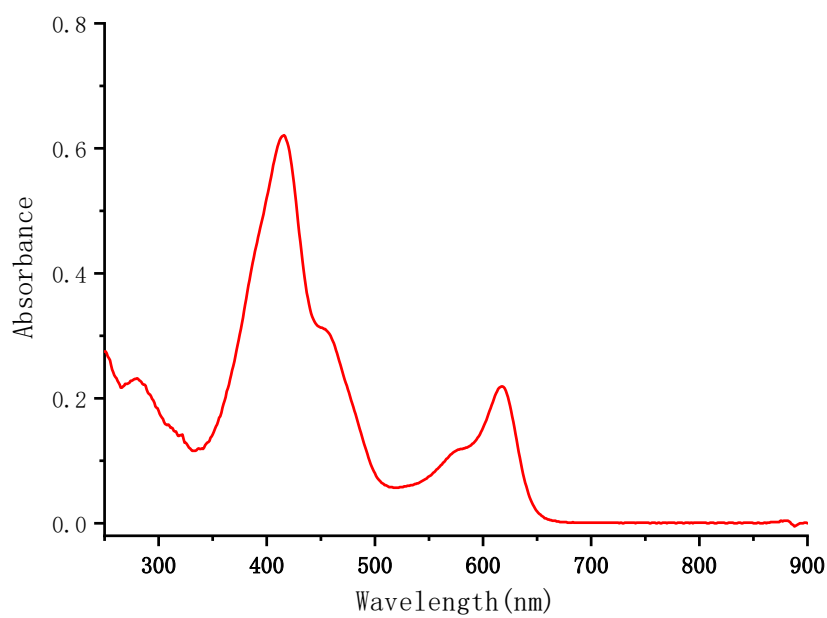


**Figure S38.** UV-vis spectrum of **3b** ( $\text{CH}_2\text{Cl}_2$ ).

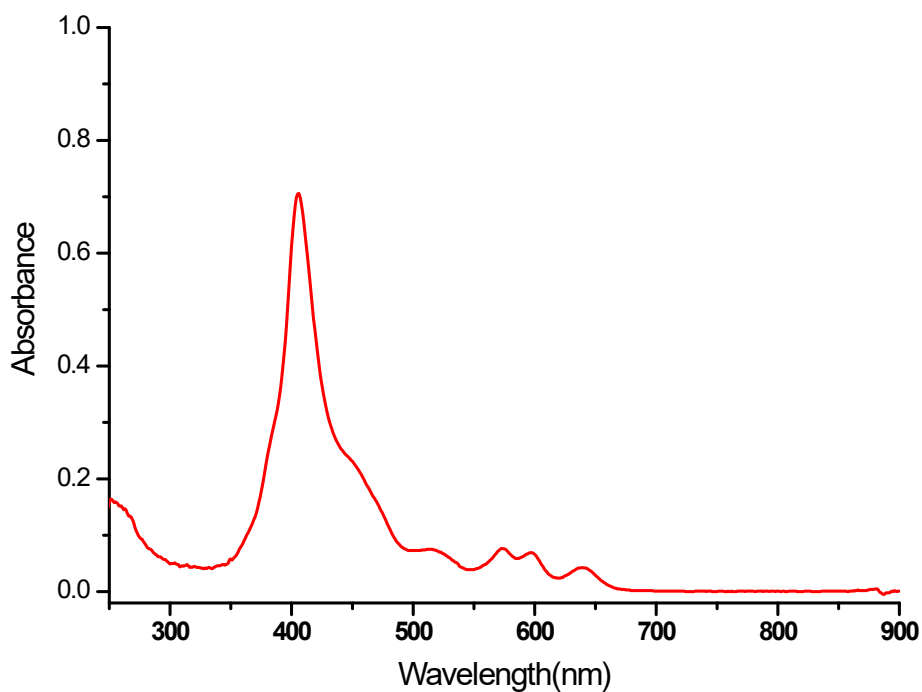


**Figure S39.** UV-vis spectrum of **4a** ( $\text{CH}_2\text{Cl}_2$ ).

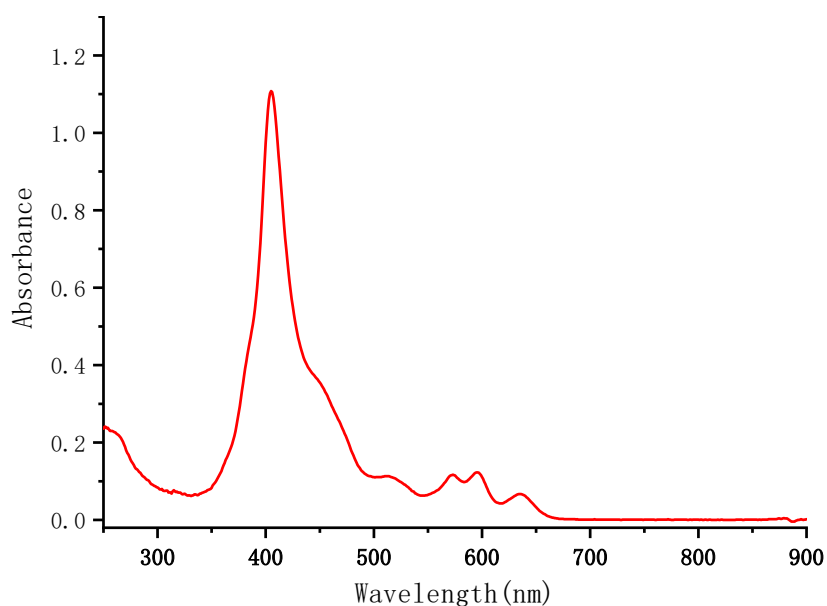


**Figure S40.** UV-vis spectrum of **4b** ( $\text{CH}_2\text{Cl}_2$ ).

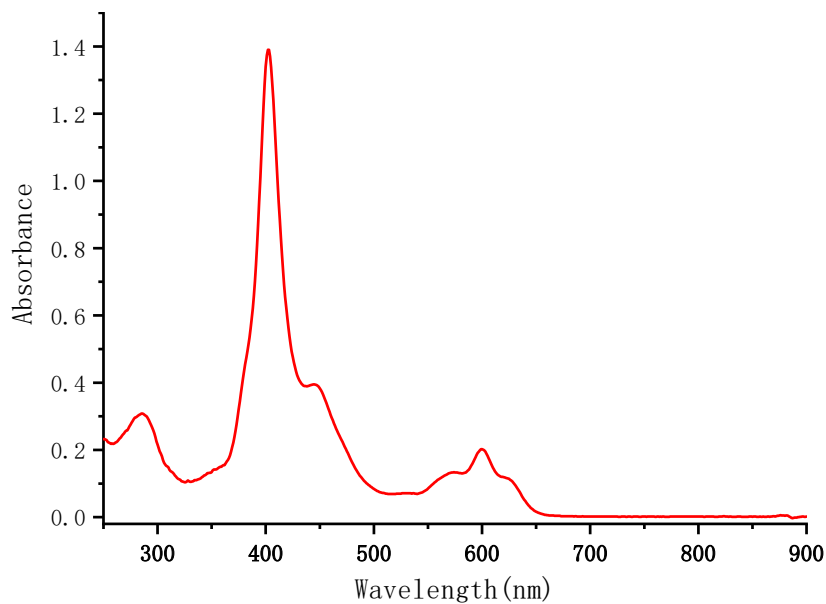


**Figure S41.** UV-vis spectrum of **5a** ( $\text{CH}_2\text{Cl}_2$ ).

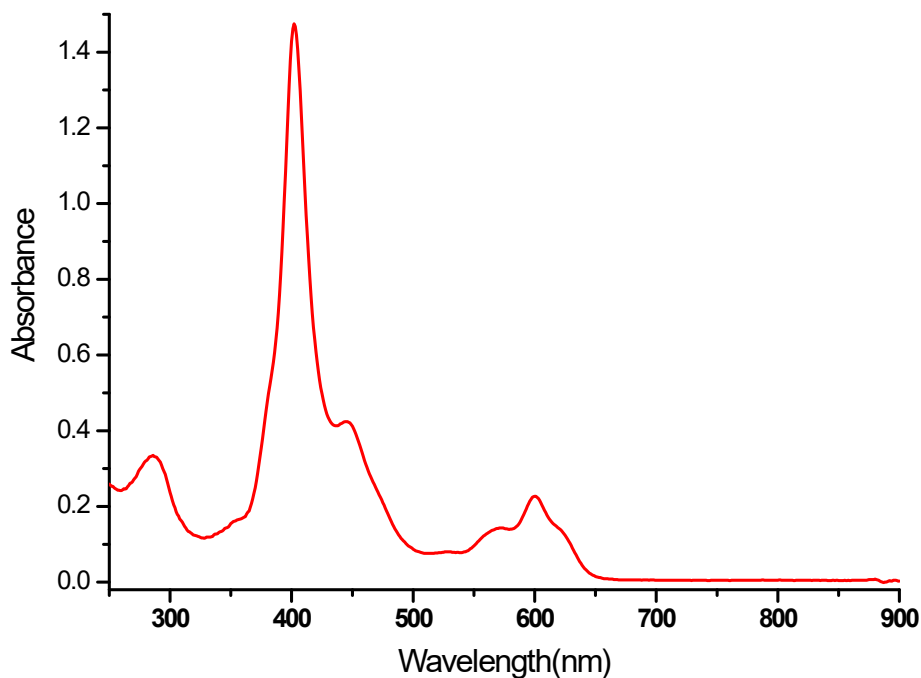


**Figure S42.** UV-vis spectrum of **5b** ( $\text{CH}_2\text{Cl}_2$ ).

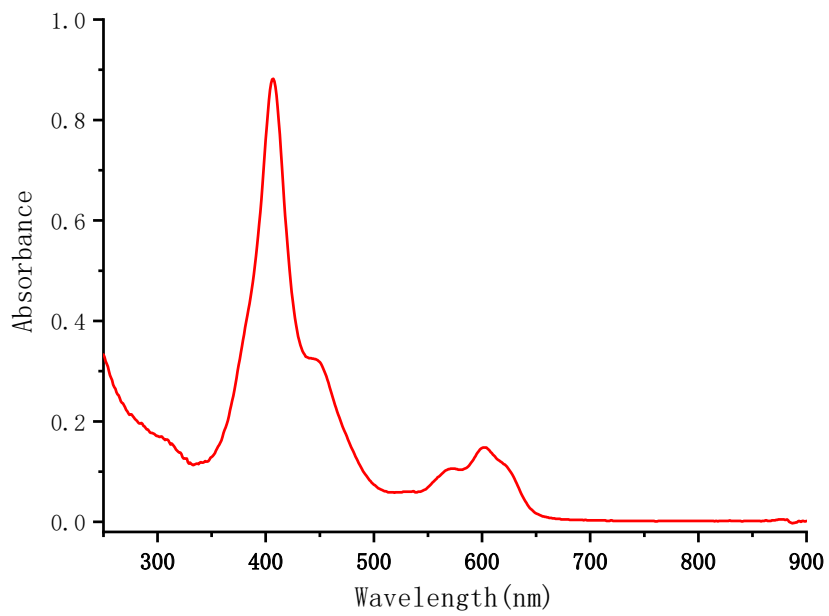


**Figure S43.** UV-vis spectrum of **5c** ( $\text{CH}_2\text{Cl}_2$ ).

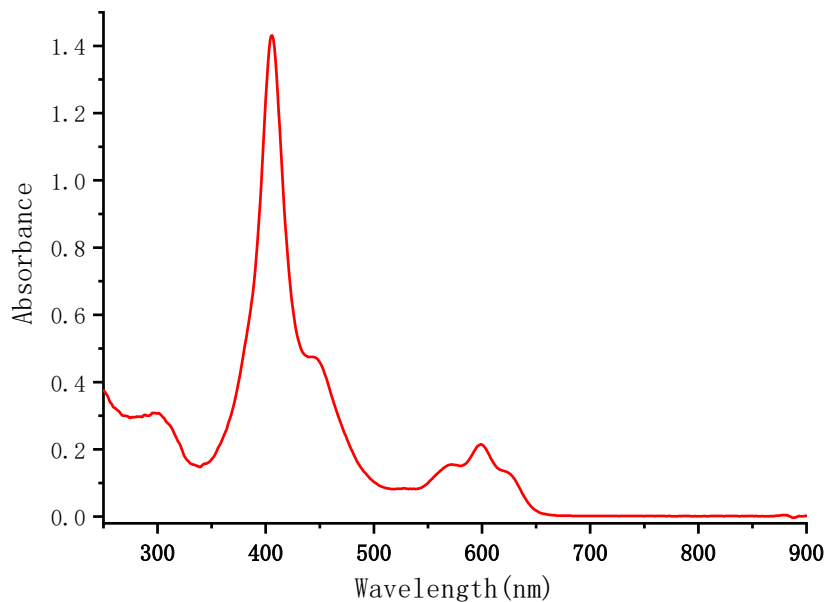


**Figure S44.** UV-vis spectrum of **5d** ( $\text{CH}_2\text{Cl}_2$ ).

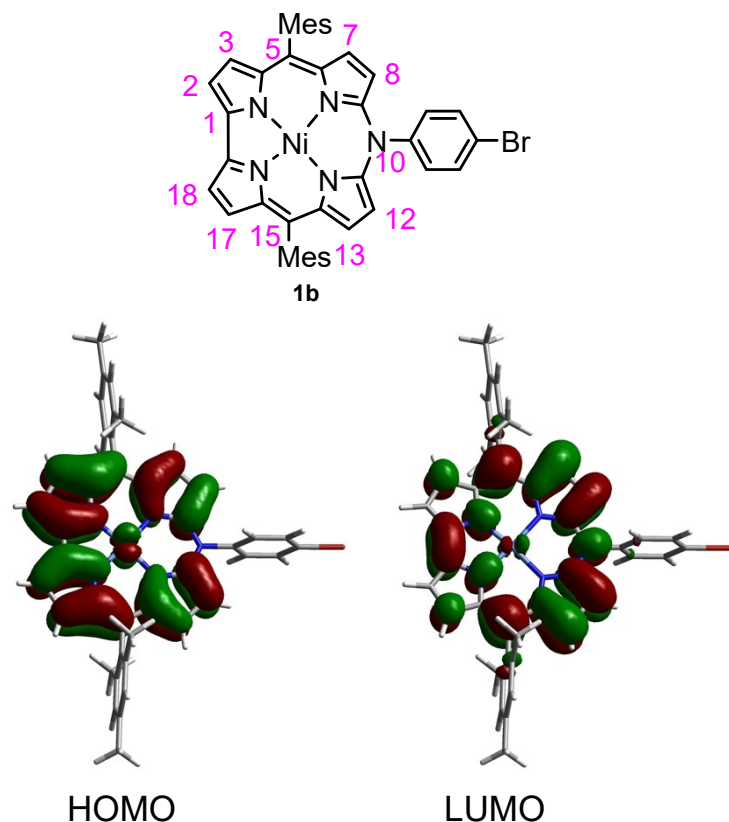


**Figure S45.** Kohn-Sham frontier orbital distributions in **1a** (isosurface 0.02).

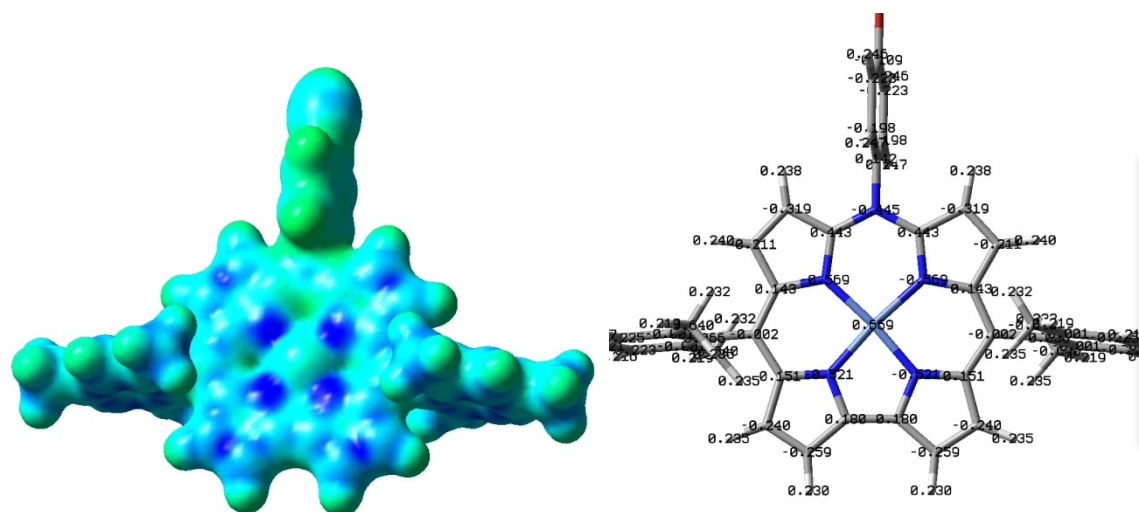


**Figure S46.** Electrostatic potential and charge distribution in **1a** calculated by NBO approach.

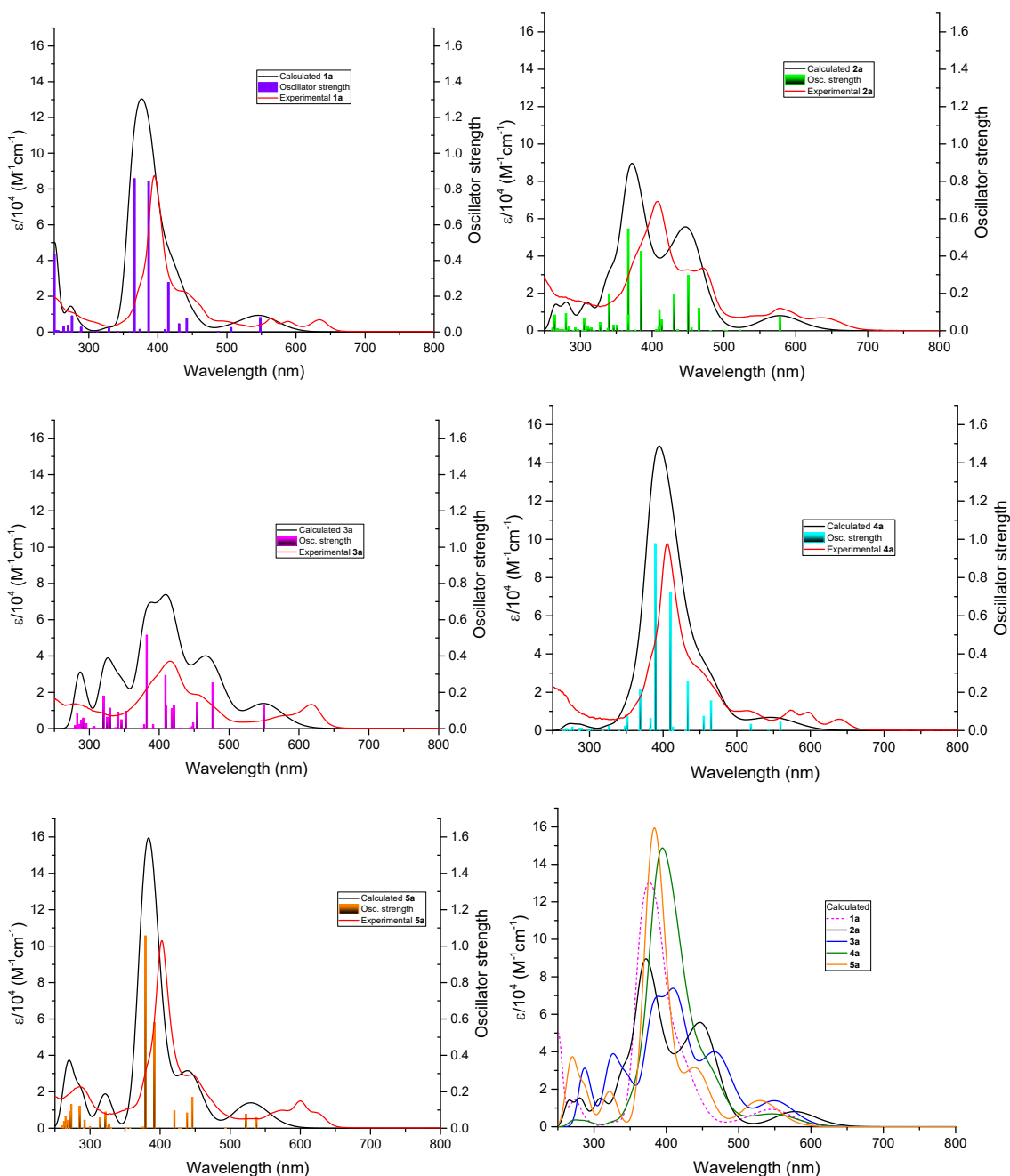


**Figure S47** Calculated (black traces) and experimental (red traces) UV-Vis spectra along with histograms representing oscillator strengths of the transitions obtained by TD DFT for DFT-optimized models of the substituted azacorroles **1a-5a**.

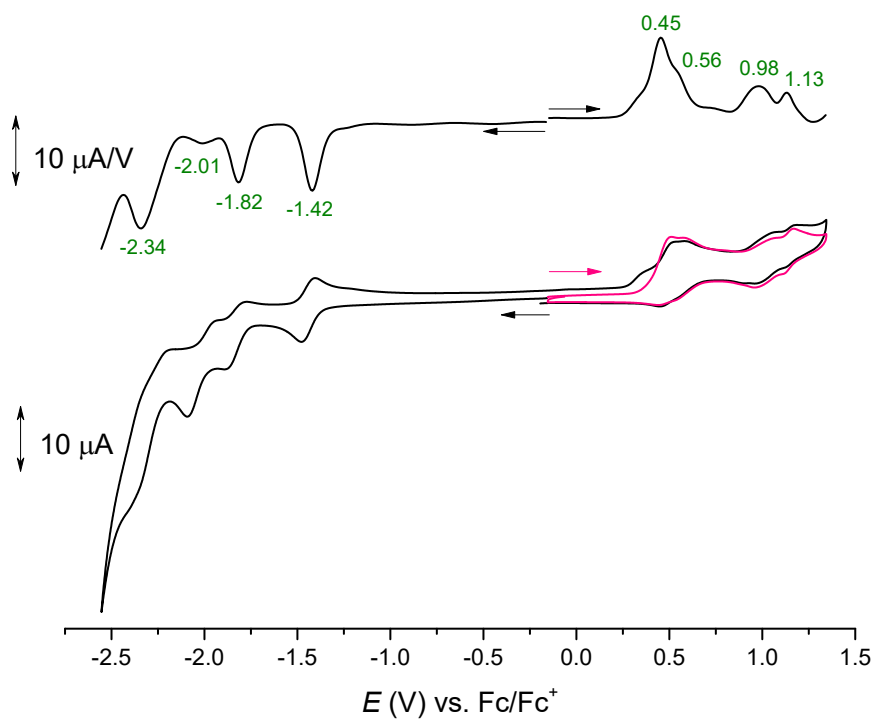


**Figure S48** Cyclic (lower traces) and differential pulse (upper traces) voltammograms for **2a** in dichloromethane solution. The green numbers are the electrode potentials in volts. The horizontal arrows indicate directions of the potential advances.

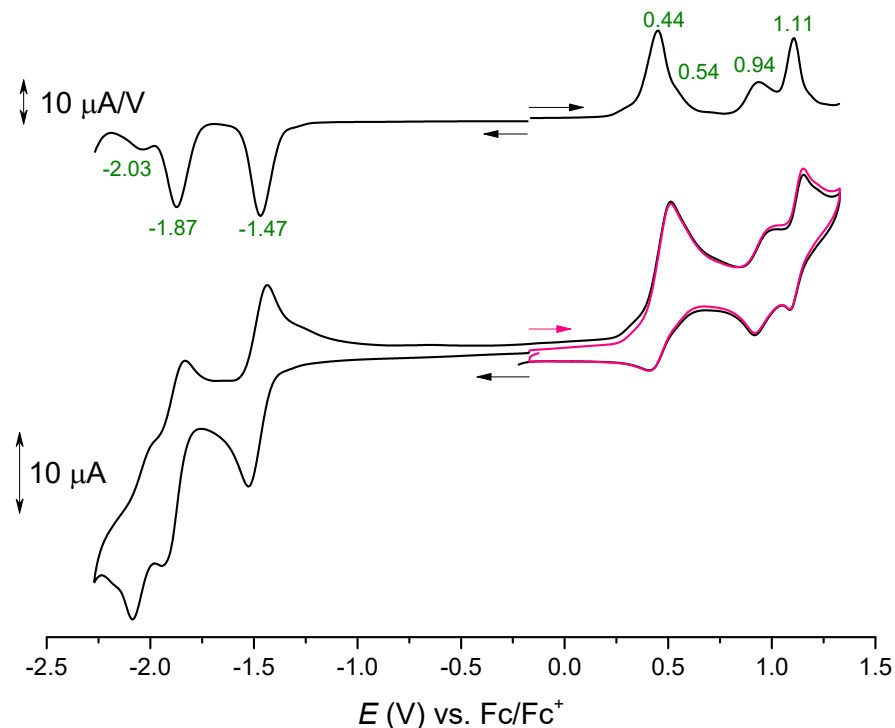


**Figure S49** Cyclic (lower traces) and differential pulse (upper traces) voltammograms for **2b** in dichloromethane solution. The green numbers are the electrode potentials in volts. The horizontal arrows indicate directions of the potential advances.

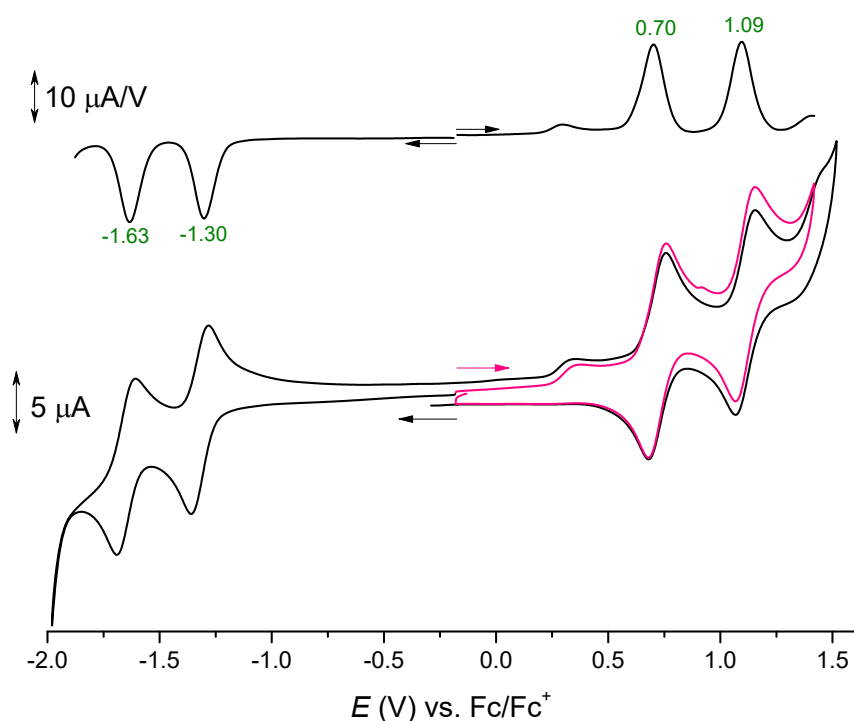


**Figure S50** Cyclic (lower traces) and differential pulse (upper traces) voltammograms for **3a** in dichloromethane solution. The green numbers are the electrode potentials in volts. The horizontal arrows indicate directions of the potential advances.

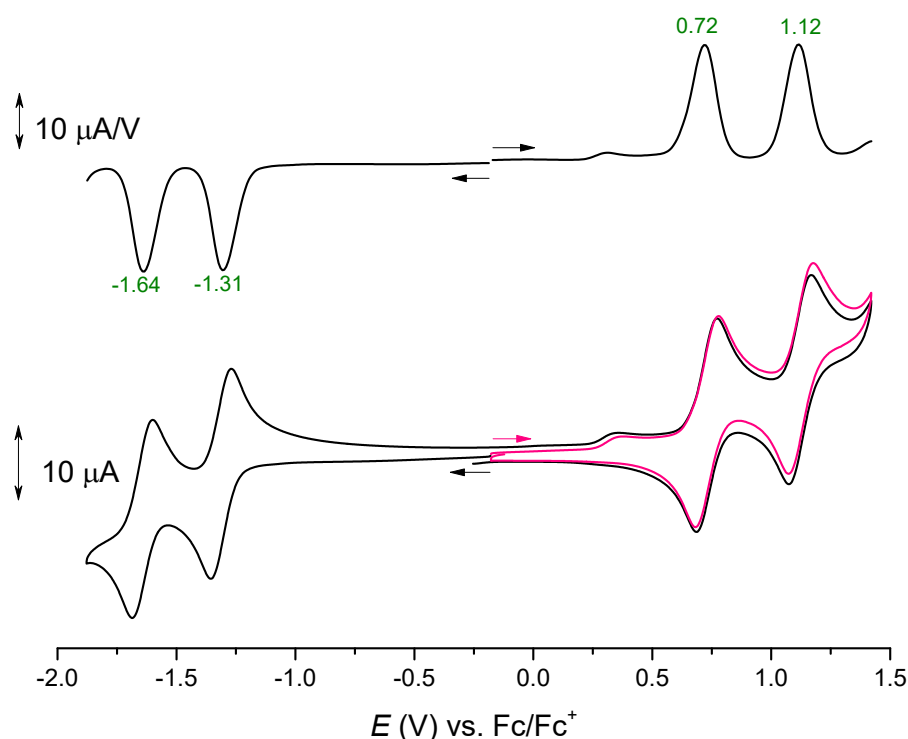


**Figure S51** Cyclic (lower traces) and differential pulse (upper traces) voltammograms for **3b** in dichloromethane solution. The green numbers are the electrode potentials in volts. The horizontal arrows indicate directions of the potential advances.

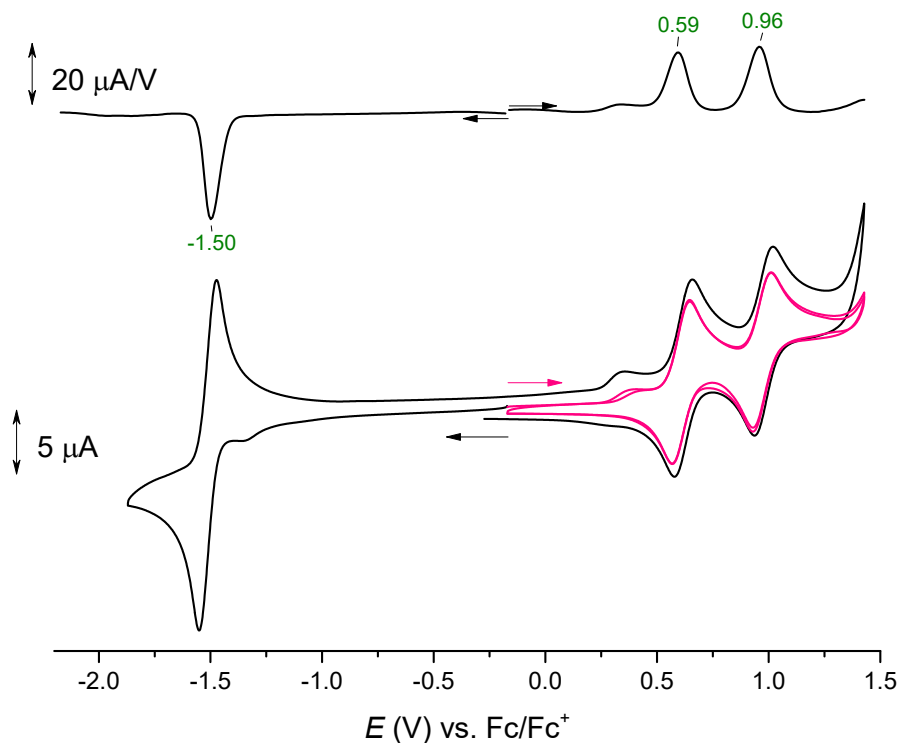


**Figure S52** Cyclic (lower traces) and differential pulse (upper traces) voltammograms for **4a** in dichloromethane solution. The green numbers are the electrode potentials in volts. The horizontal arrows indicate directions of the potential advances.

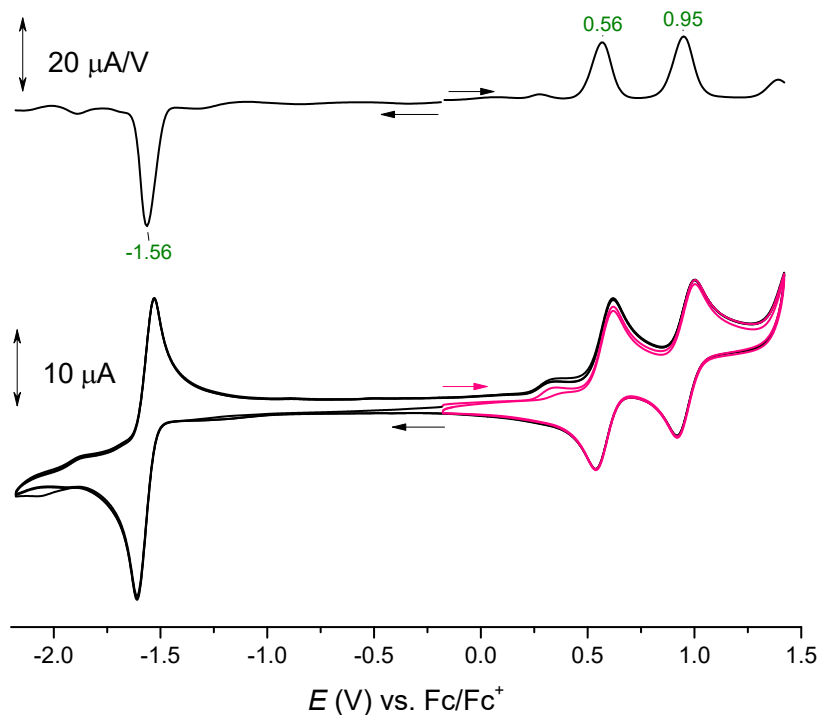


**Figure S53** Cyclic (lower traces) and differential pulse (upper traces) voltammograms for **4b** in dichloromethane solution. The green numbers are the electrode potentials in volts. The horizontal arrows indicate directions of the potential advances.

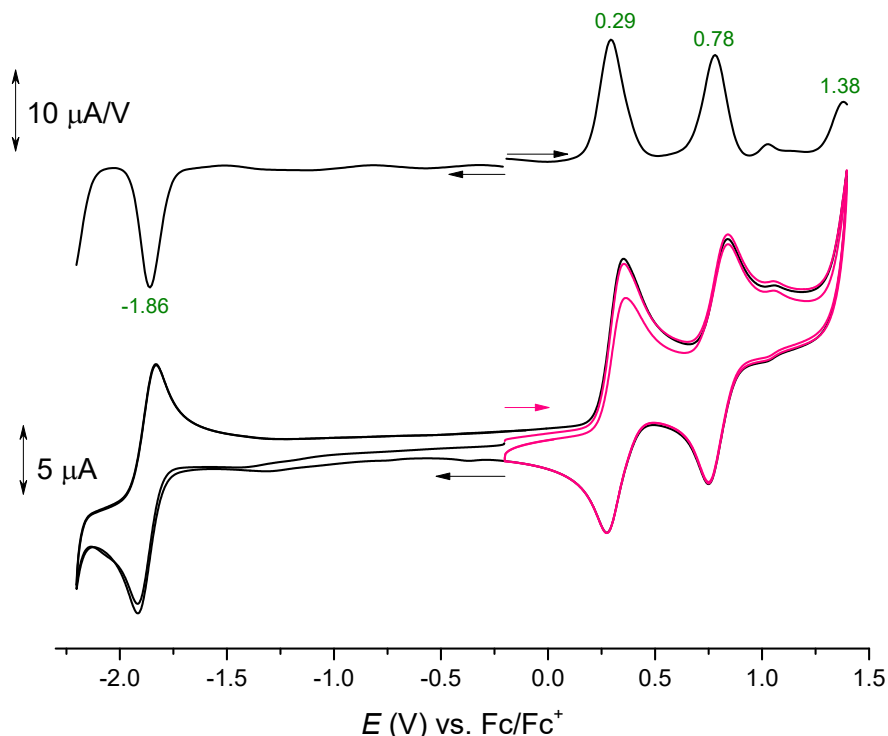


**Figure S54** Cyclic (lower traces) and differential pulse (upper traces) voltammograms for **5a** in dichloromethane solution. The green numbers are the electrode potentials in volts. The horizontal arrows indicate directions of the potential advances.

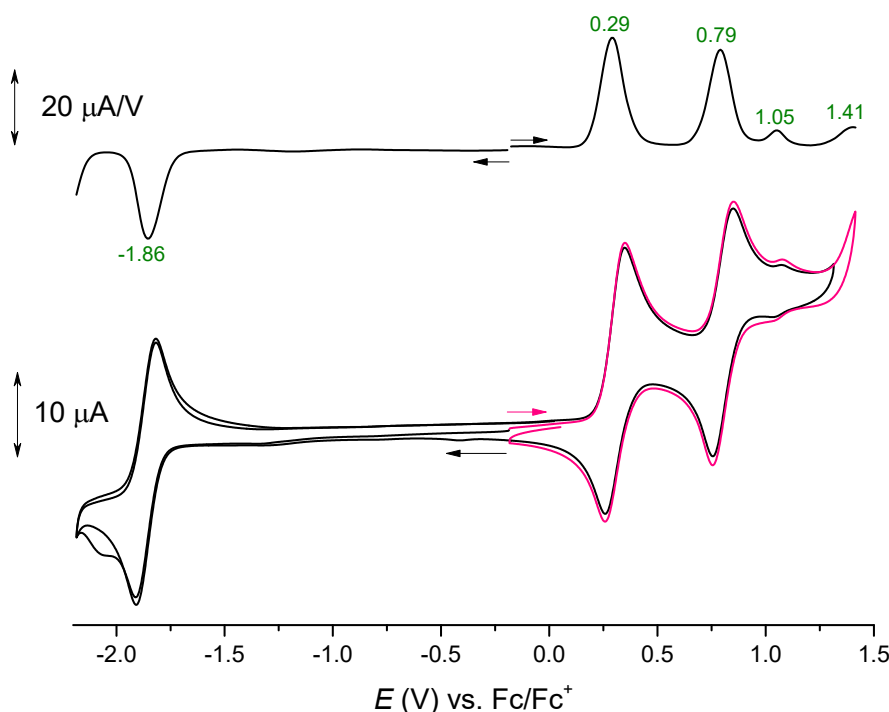


**Figure S55** Cyclic (lower traces) and differential pulse (upper traces) voltammograms for **5b** in dichloromethane solution. The green numbers are the electrode potentials in volts. The horizontal arrows indicate directions of the potential advances.

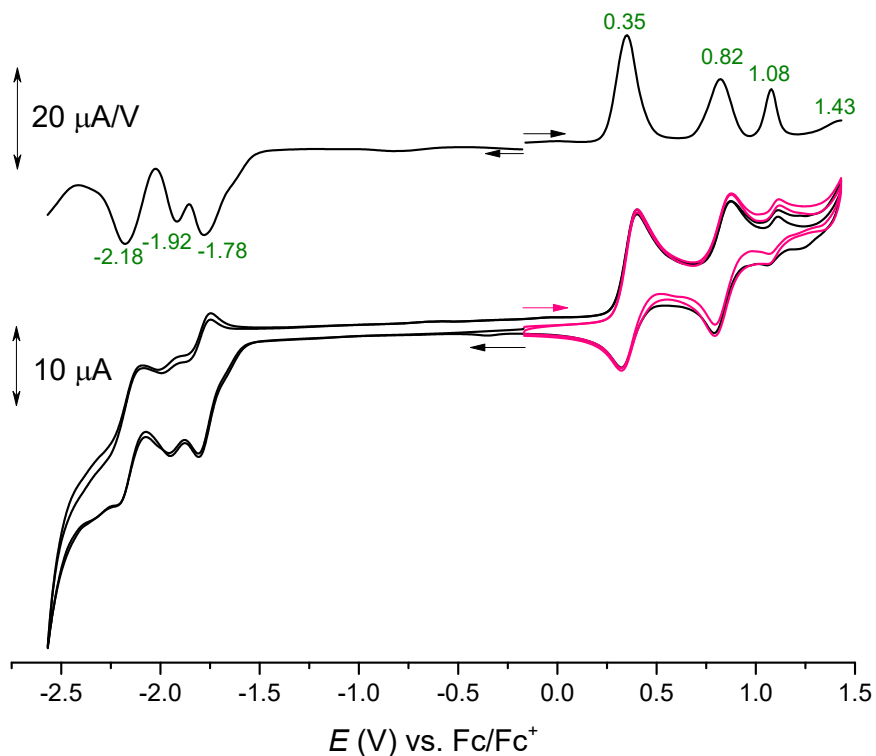


**Figure S56** Cyclic (lower traces) and differential pulse (upper traces) voltammograms for **5c** in dichloromethane solution. The green numbers are the electrode potentials in volts. The horizontal arrows indicate directions of the potential advances.

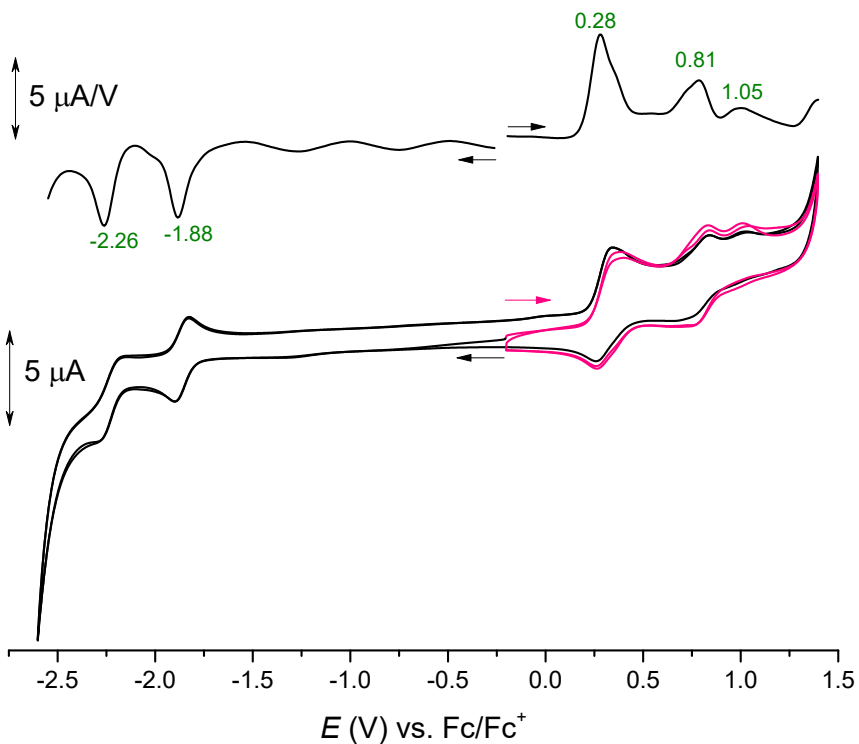


**Figure S57** Cyclic (lower traces) and differential pulse (upper traces) voltammograms for **5d** in dichloromethane solution. The green numbers are the electrode potentials in volts. The horizontal arrows indicate directions of the potential advances.

**Table S1.** Electrochemical data for the 10-azacorrole derivatives (DCM, electrode potentials in V vs. Fc/Fc<sup>+</sup>)

Entry	Compd.	$E_{\text{Red}3}$	$E_{\text{Red}2}$	$E_{\text{Red}1}$	$E_{\text{Ox}1}$	$E_{\text{Ox}2}$	$E_{\text{Ox}3}$	$\Delta E$
1	<b>2a</b>	-2.01 <sup>[a]</sup>	-1.82	-1.42	0.45	0.98	1.13	1.87
2	<b>2b</b>	-2.03 <sup>[a]</sup>	-1.87	-1.47	0.44	0.94	1.11	1.91
3	<b>3a</b>	-	-1.63	-1.30	0.70	1.09	-	2.00
4	<b>3b</b>	-	-1.64	-1.31	0.72	1.12	-	2.03
5	<b>4a</b>	-	-	-1.50	0.59	0.96		2.09
6	<b>4b</b>	-	-	-1.56	0.56	0.95		2.12
7	<b>5a</b>	-	-	-1.86	0.29	0.78	1.38 <sup>[a]</sup>	2.15
8	<b>5b</b>	-	-	-1.86	0.29	0.79	1.41 <sup>[a]</sup>	2.15
9	<b>5c</b>	-2.18	-1.92 <sup>[a]</sup>	-1.78	0.35	0.82	1.08 <sup>[a]</sup>	2.13
10	<b>5d</b>		-2.26	-1.88	0.28	0.91	1.05 <sup>[a]</sup>	2.16
11	<b>1(3-Me)<sup>[b]</sup></b>			-2.09	0.16	0.68		2.25
12	<b>1(3-F)<sup>[c]</sup></b>			-2.07	0.10	0.69		2.17
13	<b>1(4-Br)<sup>[d]</sup></b>			-2.08	0.18	0.68		2.26

[a] Irreversible couple. [b] Data from *Chem. Commun.*, 2023, **59**, 3739 (ref. <sup>45</sup>) for *N*-(3-methylphenyl)-10-azacorrole. [c] Data from *Chem. Commun.*, 2023, **59**, 3739 (ref. <sup>45</sup>) for *N*-(3-fluorophenyl)-10-azacorrole. [d] Data from *Chem. Commun.*, 2023, **59**, 3739 (ref. <sup>45</sup>) for *N*-(4-bromophenyl)-10-azacorrole.

**Table S2** Electronic transitions calculated for **1a**

No.	Energy (cm <sup>-1</sup> )	Wavelength (nm)	Osc. Strength	Major contribs
1	18235.4	548.4	0.0801	HOMO->LUMO (87%)
2	19754.9	506.2	0.0246	H-1->LUMO (23%), HOMO->L+1 (72%)
3	19925.9	501.9	0	H-3->L+4 (51%), HOMO->L+4 (33%)
4	20520.4	487.3	0.0019	H-4->L+4 (91%)
5	21090.6	474.1	0	H-15->L+4 (10%), H-2->L+4 (83%)
6	22632.7	441.8	0.0768	H-2->LUMO (66%), H-1->LUMO (25%)
7	23049.7	433.8	0.0003	H-4->LUMO (99%)
8	23217.5	430.7	0.0454	H-3->LUMO (40%), H-1->L+1 (53%) H-3->L+1 (29%), H-2->LUMO (29%), H-1->LUMO (29%), HOMO->L+1 (13%)
9	24084.5	415.2	0.2764	
10	24365.2	410.4	0.0136	H-2->L+1 (90%)
11	24757.2	403.9	0	H-4->L+1 (99%)
12	25863.8	386.6	0.8422	H-3->LUMO (45%), H-1->L+1 (38%)
13	26746.2	373.9	0.0146	H-17->L+4 (94%)
14	27311.5	366.1	0.8567	H-3->L+1 (62%), H-1->LUMO (22%), HOMO->L+1 (14%)
15	27818.1	359.5	0.0001	H-6->L+1 (26%), H-5->LUMO (73%)
16	27836.6	359.2	0	H-6->LUMO (72%), H-5->L+1 (27%)
17	28875.5	346.3	0	HOMO->L+2 (99%)
18	29245.7	341.9	0.0003	H-8->LUMO (44%), H-7->LUMO (33%), H-7->L+1 (21%)
19	29247.3	341.9	0.0007	H-8->LUMO (33%), H-8->L+1 (20%), H-7->LUMO (44%)
20	30232.9	330.8	0	H-3->L+4 (29%), HOMO->L+4 (66%)
21	30381.3	329.1	0.0225	H-9->LUMO (98%)
22	30475.7	328.1	0.0002	HOMO->L+3 (99%)
23	30962.8	323.0	0	H-1->L+2 (92%)
24	31005.6	322.5	0	H-6->LUMO (27%), H-5->L+1 (73%)
25	31031.4	322.3	0	H-6->L+1 (74%), H-5->LUMO (26%)
26	31266.1	319.8	0	H-1->L+4 (92%)
27	31960.5	312.9	0	H-8->L+1 (49%), H-7->LUMO (19%), H-7->L+1 (26%)
28	31964.6	312.8	0.0002	H-8->LUMO (20%), H-8->L+1 (27%), H-7->L+1 (51%)
29	32067.8	311.8	0.0026	H-9->L+1 (94%)
30	32613.0	306.6	0.0022	H-1->L+3 (99%)
31	33888.2	295.1	0	H-10->LUMO (99%)
32	34610.1	288.9	0.0264	H-11->LUMO (97%)
33	34829.4	287.1	0.0003	HOMO->L+5 (97%)
34	34859.3	286.9	0.0001	HOMO->L+6 (97%)
35	35433.5	282.2	0	H-2->L+2 (99%)
36	35744.9	279.8	0	H-3->L+2 (98%)
37	36269.9	275.7	0.0897	H-11->L+1 (85%)
38	36293.3	275.5	0.0008	H-10->L+1 (96%)
39	36507.1	273.9	0	H-17->LUMO (97%)

40	36747.4	272.1	0	H-4->L+2 (100%)
41	36814.4	271.6	0.0044	HOMO->L+8 (91%)
42	36844.2	271.4	0.0017	H-2->L+3 (94%)
43	36846.6	271.4	0.0001	HOMO->L+9 (93%)
44	37053.1	269.9	0.0366	H-13->LUMO (25%), H-12->LUMO (51%)
45	37199.9	268.8	0	H-3->L+3 (98%)
46	37636.2	265.7	0.0003	H-15->LUMO (58%), H-14->LUMO (36%)
47	37779.0	264.7	0	HOMO->L+7 (99%)
48	37790.3	264.6	0.0001	H-1->L+5 (96%)
49	37816.9	264.4	0	H-16->LUMO (25%), H-13->LUMO (25%), H-12->LUMO (34%), HOMO->L+10 (10%)
50	37950.0	263.5	0.032	H-4->L+3 (100%)
51	38146.8	262.1	0	H-17->L+1 (99%)
52	38313.8	261.0	0	H-16->L+1 (15%), H-15->LUMO (11%), H-13->L+1 (59%)
53	38569.4	259.3	0.0001	H-15->LUMO (14%), H-14->LUMO (32%), H-12->L+1 (49%)
54	39091.3	255.8	0.0066	H-16->LUMO (55%), H-13->LUMO (19%), HOMO->L+10 (23%)
55	39358.2	254.1	0.0023	H-15->L+1 (41%), H-14->L+1 (50%)
56	39519.6	253.0	0.0083	H-1->L+8 (95%)
57	39813.9	251.2	0.0017	H-1->L+9 (93%)
58	39824.4	251.1	0.0075	H-15->L+1 (13%), H-13->LUMO (15%), HOMO->L+10 (50%)
59	39980.1	250.1	0.4369	H-1->L+7 (99%)
60	40381.8	247.6	0.0001	

**Table S3** Electronic transitions calculated for **2a**

No.	Energy (cm <sup>-1</sup> )	Wavelength (nm)	Osc. Strength	Major contribs
1	17311.1	577.7	0.0738	HOMO->LUMO (92%)
2	19140.3	522.5	0.0038	H-1->LUMO (36%), HOMO->L+1 (60%)
3	19841.2	504.0	0.0008	H-3->L+4 (19%), H-2->L+4 (18%), HOMO->L+4 (19%)
4	19952.5	501.2	0.0027	H-5->L+4 (56%), H-5->L+5 (24%)
5	20772.8	481.4	0.0005	H-3->L+4 (23%), H-3->L+5 (10%), H-2->L+4 (29%), H-2->L+5 (13%)
6	21510.8	464.9	0.1214	H-2->LUMO (58%), H-1->LUMO (13%), HOMO->L+1 (10%)
7	21990.7	454.7	0.0148	H-5->LUMO (79%)
8	22203.6	450.4	0.2951	H-2->LUMO (20%), H-1->LUMO (28%), H-1->L+1 (14%), HOMO->L+1 (10%)
9	22965.8	435.4	0.0049	H-4->LUMO (81%)
10	23219.9	430.7	0.1959	H-3->LUMO (45%), H-1->L+1 (15%)
11	24224.9	412.8	0.0568	H-3->LUMO (21%), H-3->L+1 (11%), H-2->L+1 (43%), H-1->L+1 (13%)
12	24388.6	410.0	0.1124	H-2->L+1 (31%), H-1->L+1 (19%), HOMO->L+2 (24%)
13	24445.1	409.1	0.0198	H-5->L+1 (86%)
14	24648.3	405.7	0.0067	H-6->LUMO (97%)
15	25980.7	384.9	0.4233	H-3->L+1 (57%), H-2->L+1 (16%)
16	26568.7	376.4	0.0028	H-17->L+4 (60%), H-17->L+5 (26%)
17	26942.1	371.2	0.0002	H-7->LUMO (25%), H-7->L+1 (73%)
18	27266.4	366.8	0.5457	H-7->LUMO (10%), H-1->L+1 (15%), HOMO->L+2 (48%)
19	27274.4	366.6	0.0838	H-7->LUMO (64%), H-7->L+1 (22%)

20	27962.4	357.6	0.0002	H-8->LUMO (95%)
21	28427.8	351.8	0.0011	H-8->L+1 (88%)
22	28456.9	351.4	0.0296	H-4->L+1 (84%)
23	28901.3	346.0	0.0305	H-9->LUMO (83%)
24	29402.1	340.1	0.1978	H-1->L+2 (73%)
25	29578.0	338.1	0.0124	H-3->L+4 (10%), HOMO->L+4 (45%), HOMO->L+5 (19%)
26	29711.0	336.6	0.0002	H-6->L+1 (99%)
27	30326.4	329.7	0.0006	HOMO->L+3 (96%)
28	30538.6	327.5	0.0423	H-13->LUMO (10%), H-11->LUMO (24%), H-4->L+2 (11%)
29	31299.2	319.5	0.0016	H-1->L+4 (64%), H-1->L+5 (27%)
30	31390.3	318.6	0.0002	H-10->LUMO (96%)
31	31754.9	314.9	0.0162	H-9->L+1 (93%)
32	31971.0	312.8	0.0135	H-2->L+2 (10%), HOMO->L+4 (27%), HOMO->L+5 (59%)
33	32222.7	310.3	0.0264	H-4->L+2 (19%), H-3->L+2 (27%), H-2->L+2 (42%)
34	32276.7	309.8	0.0188	H-4->L+2 (36%), H-3->L+2 (12%), H-2->L+2 (32%)
35	32730.0	305.5	0.0639	H-11->LUMO (24%), H-4->L+2 (20%), H-3->L+2 (39%)
36	32796.9	304.9	0.0016	H-1->L+3 (95%)
37	33060.7	302.5	0.0025	H-5->L+2 (97%)
38	33737.4	296.4	0.0048	H-6->L+2 (95%)
39	34149.5	292.8	0.0051	H-10->L+1 (72%) H-13->LUMO (13%), H-12->LUMO (13%), H-11->LUMO (28%), H-10->L+1 (25%)
40	34151.9	292.8	0.0141	H-1->L+4 (29%), H-1->L+5 (68%) H-21->LUMO (15%), H-20->LUMO (14%), H-17->LUMO (12%), H-12->LUMO (16%)
41	34489.1	289.9	0.0011	H-16->LUMO (15%), H-12->LUMO (23%), H-11->L+1 (30%)
42	35187.6	284.2	0.0194	H-13->LUMO (12%), H-12->LUMO (15%), H-11->L+1 (48%)
43	35330.3	283.0	0.0133	H-17->LUMO (66%)
44	35727.1	279.9	0.0913	H-16->LUMO (10%), H-14->LUMO (62%)
45	35893.3	278.6	0.0029	H-11->L+1 (30%)
46	36198.2	276.3	0.0001	HOMO->L+6 (98%)
47	36259.5	275.8	0.006	H-15->LUMO (61%), H-12->LUMO (12%)
48	36724.8	272.3	0.0003	H-7->L+2 (94%)
49	36733.7	272.2	0	H-2->L+3 (98%)
50	36743.4	272.2	0.0057	H-19->LUMO (14%), H-14->LUMO (10%), H-13->LUMO (35%), H-13->L+1 (11%)
51	37306.4	268.1	0.0001	H-8->L+2 (99%)
52	37323.3	267.9	0.0093	HOMO->L+7 (94%)
53	37486.2	266.8	0.0001	H-17->L+1 (43%), H-12->L+1 (15%)
54	37493.5	266.7	0.0049	H-16->LUMO (33%), H-15->LUMO (13%), H-12->L+1 (19%)
55	37781.4	264.7	0.0844	H-17->L+1 (19%), H-12->L+1 (26%), HOMO->L+9 (31%)
56	38075.8	262.6	0.0041	H-5->L+3 (97%)
57	38212.9	261.7	0	H-2->L+4 (12%), H-2->L+5 (29%), HOMO->L+9 (41%)
58	38223.4	261.6	0.0051	H-17->L+1 (19%), H-2->L+4 (15%), H-2->L+5 (32%), HOMO->L+9 (12%)
59	38264.6	261.3	0.0032	
60	38277.5	261.3	0.0138	

**Table S4** Electronic transitions calculated for **3a**

No.	Energy (cm <sup>-1</sup> )	Wavelength (nm)	Osc. Strength	Major contribs
1	18187.8	549.8	0.1248	H-1->L+1 (10%), HOMO->LUMO (86%)
2	18578.2	538.3	0.0015	H-1->LUMO (13%), HOMO->L+1 (80%)
3	19512.2	512.5	0.0013	H-8->L+4 (77%)
4	19834.8	504.2	0.0004	H-5->L+4 (49%), HOMO->L+4 (23%)
5	20522.8	487.3	0.0013	H-4->L+4 (67%)
6	20991.4	476.4	0.2517	H-1->LUMO (71%), HOMO->L+1 (10%)
7	22008.5	454.4	0.1437	H-5->LUMO (19%), H-4->L+1 (11%), H-2->LUMO (19%), H-1->L+1 (37%)
8	22251.2	449.4	0.0009	H-8->LUMO (57%), H-4->LUMO (17%), H-3->LUMO (14%)
9	22294.0	448.6	0.0318	H-5->LUMO (10%), H-3->L+1 (22%), H-2->LUMO (50%), H-1->L+1 (13%)
10	22361.7	447.2	0.0114	H-8->LUMO (24%), H-3->LUMO (46%), H-2->L+1 (19%)
11	22506.9	444.3	0.0053	H-8->LUMO (12%), H-4->LUMO (63%)
12	23242.5	430.2	0.0015	H-8->L+1 (96%)
13	23747.4	421.1	0.1254	H-7->LUMO (33%), H-6->L+1 (10%), H-4->L+1 (34%)
14	23836.9	419.5	0.001	H-7->L+1 (25%), H-6->LUMO (68%)
15	23926.4	417.9	0.1088	H-7->LUMO (27%), H-6->L+1 (17%), H-4->L+1 (33%)
16	24416.8	409.6	0.1253	H-5->L+1 (56%), HOMO->L+2 (17%)
17	24456.3	408.9	0.2932	H-5->LUMO (53%), H-1->L+1 (17%)
18	25483.9	392.4	0.0003	H-3->LUMO (30%), H-2->L+1 (60%)
19	25559.7	391.2	0.0207	H-3->L+1 (64%), H-2->LUMO (27%)
20	26171.9	382.1	0.5148	H-5->L+1 (14%), HOMO->L+2 (72%)
21	26418.7	378.5	0.0216	H-18->L+4 (71%)
22	26609.8	375.8	0.0008	H-7->L+1 (24%), H-6->LUMO (19%), H-6->L+1 (45%)
23	26613.1	375.8	0.0008	H-7->LUMO (18%), H-7->L+1 (44%), H-6->L+1 (25%)
24	28380.2	352.4	0.096	H-1->L+2 (21%), HOMO->L+3 (68%)
25	28904.5	346.0	0.0491	H-10->LUMO (33%), H-1->L+2 (56%)
26	29290.0	341.4	0.0911	H-10->LUMO (43%), H-1->L+2 (14%)
27	29645.7	337.3	0.0052	H-5->L+4 (17%), HOMO->L+4 (70%)
28	29679.6	336.9	0.001	H-11->LUMO (13%), H-10->L+1 (47%)
29	30374.0	329.2	0.113	H-10->L+1 (14%), H-1->L+3 (34%), H-1->L+4 (31%)
30	30621.6	326.6	0	H-10->L+1 (26%), H-2->L+2 (10%), H-1->L+4 (41%)
31	30636.2	326.4	0.0006	H-9->LUMO (99%)
32	30688.6	325.9	0.0635	H-11->L+1 (10%), H-10->LUMO (15%), H-3->L+2 (26%)
33	30909.6	323.5	0.0001	H-9->L+1 (99%)
34	31178.2	320.7	0.1776	H-1->L+3 (41%), H-1->L+4 (21%)
35	31699.2	315.5	0.0009	H-11->LUMO (15%), H-3->L+3 (11%), H-2->L+2 (46%), H-1->L+3 (12%)
36	31844.4	314.0	0.0034	H-4->L+2 (27%), H-3->L+2 (31%), H-2->L+3 (18%)
37	32266.2	309.9	0.0001	HOMO->L+5 (97%)
38	32542.9	307.3	0.0097	H-11->LUMO (17%), H-5->L+2 (70%)
39	32597.7	306.8	0.0121	H-6->L+2 (22%), H-4->L+2 (42%)
40	32716.3	305.7	0.0067	H-7->L+2 (73%), H-6->L+3 (20%)
41	32801.0	304.9	0.0002	H-7->L+3 (12%), H-6->L+2 (50%), H-4->L+2 (11%)

42	33235.7	300.9	0.0002	H-8->L+2 (98%)
43	33820.4	295.7	0.0268	H-11->LUMO (10%), H-5->L+2 (11%), H-4->L+3 (60%)
44	33894.6	295.0	0.0001	H-1->L+5 (96%)
45	33962.4	294.4	0.0168	HOMO->L+6 (90%)
46	34328.6	291.3	0.0584	H-11->L+1 (17%), H-5->L+3 (54%)
47	34701.2	288.2	0.0246	H-12->LUMO (28%), H-11->L+1 (32%), H-5->L+3 (12%) H-14->LUMO (28%), H-12->L+1 (14%), H-11->LUMO (17%), H-4->L+3
48	34706.8	288.1	0.0471	(14%)
49	34784.3	287.5	0.0027	H-8->L+3 (77%) H-21->LUMO (10%), H-12->LUMO (20%), H-3->L+2 (14%), H-2->L+3
50	34994.8	285.8	0.0097	(15%)
51	35064.1	285.2	0.0208	H-12->L+1 (18%), H-8->L+3 (18%)
52	35256.1	283.6	0.0235	H-3->L+2 (11%), H-2->L+3 (47%)
53	35276.3	283.5	0.0022	H-3->L+3 (58%), H-2->L+2 (15%)
54	35358.5	282.8	0.0121	H-13->LUMO (11%), H-12->LUMO (37%)
55	35377.1	282.7	0.0832	H-14->LUMO (14%), H-12->L+1 (52%)
56	35713.4	280.0	0.0165	H-1->L+6 (93%)
57	36094.9	277.0	0.0014	H-15->LUMO (45%), H-14->L+1 (24%), H-13->LUMO (11%)
58	36119.9	276.9	0.0006	H-15->L+1 (14%), H-14->LUMO (22%), H-13->L+1 (29%)
59	36283.7	275.6	0.0002	H-7->L+3 (58%), H-6->L+2 (23%), H-6->L+3 (14%)
60	36290.1	275.6	0	H-7->L+2 (22%), H-7->L+3 (14%), H-6->L+3 (58%)

**Table S5** Electronic transitions calculated for **4a**

No.	Energy (cm <sup>-1</sup> )	Wavelength (nm)	Osc. Strength	Major contribs
1	17879.7	559.3	0.044	H-6->L+2 (11%), HOMO->LUMO (77%)
2	18096.7	552.6	0	H-12->L+2 (17%), H-3->L+2 (27%), HOMO->L+2 (34%)
3	18404.0	543.4	0.007	H-6->L+2 (82%), HOMO->LUMO (10%)
4	19074.2	524.3	0	H-14->L+2 (17%), H-2->L+2 (64%)
5	19258.1	519.3	0.0325	H-1->LUMO (24%), HOMO->L+1 (71%)
6	21501.9	465.1	0.1542	H-2->LUMO (52%), H-1->LUMO (36%)
7	21972.2	455.1	0.0748	H-3->LUMO (32%), H-1->L+1 (55%)
8	23051.3	433.8	0.0003	H-6->LUMO (99%)
9	23067.5	433.5	0.254	H-3->L+1 (35%), H-2->LUMO (36%), H-1->LUMO (18%), HOMO->L+1 (10%)
10	23232.8	430.4	0.0008	H-3->LUMO (12%), H-2->L+1 (82%)
11	24203.1	413.2	0.0179	H-5->L+1 (29%), H-4->LUMO (67%)
12	24227.3	412.8	0.0003	H-5->LUMO (68%), H-4->L+1 (31%)
13	24374.1	410.3	0.719	H-3->LUMO (48%), H-1->L+1 (30%)

14	24456.3	408.9	0.0001	H-6->L+1 (99%)
15	25317.7	395.0	0.0059	H-23->L+2 (83%)
16	25695.2	389.2	0.9775	H-3->L+1 (56%), H-1->LUMO (19%), HOMO->L+1 (14%)
17	26112.2	383.0	0.0638	H-8->L+1 (23%), H-7->LUMO (72%)
18	26146.1	382.5	0.0135	H-8->LUMO (72%), H-7->L+1 (25%)
19	27108.3	368.9	0.2152	H-9->LUMO (85%)
20	27209.9	367.5	0.0003	H-5->LUMO (32%), H-4->L+1 (68%)
21	27236.5	367.2	0.0029	H-5->L+1 (69%), H-4->LUMO (30%)
22	27529.3	363.2	0	H-3->L+2 (22%), HOMO->L+2 (64%)
23	27889.0	358.6	0	H-1->L+2 (98%)
24	28454.4	351.4	0.071	H-9->L+1 (39%), H-8->L+1 (45%), H-7->LUMO (11%)
25	28596.4	349.7	0.0022	H-8->LUMO (23%), H-7->L+1 (72%)
26	28707.7	348.3	0.023	H-9->L+1 (57%), H-8->L+1 (27%), H-7->LUMO (12%)
27	29254.5	341.8	0	H-10->LUMO (98%)
28	29372.3	340.5	0.0001	H-11->LUMO (92%)
29	30657.1	326.2	0.0227	H-11->L+1 (89%)
30	31381.4	318.7	0.0001	H-12->LUMO (86%)
31	31512.1	317.3	0.0002	H-10->L+1 (98%)
32	31762.1	314.8	0	HOMO->L+3 (99%)
33	32795.3	304.9	0	H-13->LUMO (99%)
34	33056.6	302.5	0	H-1->L+3 (99%)
35	33078.4	302.3	0.0096	H-12->L+1 (91%)
36	33097.8	302.1	0	H-13->L+1 (98%)
37	33418.0	299.2	0.0009	H-14->LUMO (75%), HOMO->L+4 (19%)
38	33641.4	297.3	0.0001	H-14->LUMO (17%), HOMO->L+4 (79%)
39	34202.7	292.4	0	H-9->L+2 (47%), H-3->L+2 (39%)
40	34635.1	288.7	0.0118	H-15->LUMO (71%), H-14->L+1 (24%)
41	34837.5	287.0	0.0113	H-15->LUMO (27%), H-14->L+1 (65%)
42	35019.8	285.6	0.0005	H-1->L+4 (95%)
43	35137.5	284.6	0	H-16->LUMO (95%)
44	36102.2	277.0	0.0001	H-4->L+2 (99%)
45	36154.6	276.6	0.0162	H-5->L+2 (97%)
46	36241.7	275.9	0	H-23->LUMO (14%), H-20->LUMO (14%), H-17->LUMO (58%)
47	36495.0	274.0	0.0005	H-11->L+2 (35%), H-7->L+2 (22%), H-2->L+2 (24%)

48	36562.7	273.5	0.0021	H-18->LUMO (28%), H-15->L+1 (68%)
49	36816.8	271.6	0	H-20->LUMO (33%), H-17->LUMO (11%), H-16->L+1 (45%)
50	36940.2	270.7	0	H-21->LUMO (27%), H-17->L+1 (67%)
51	37156.3	269.1	0.0094	H-19->LUMO (57%), HOMO->L+7 (33%)
52	37202.3	268.8	0	HOMO->L+5 (78%), HOMO->L+8 (10%)
53	37231.4	268.6	0.0001	HOMO->L+6 (85%)
54	37320.1	268.0	0.0096	H-18->LUMO (57%), H-15->L+1 (30%)
55	37331.4	267.9	0	H-2->L+3 (96%)
56	37566.9	266.2	0.0002	H-9->L+2 (17%), H-8->L+2 (73%)
57	37714.5	265.2	0	H-23->LUMO (60%), H-21->L+1 (13%), H-17->LUMO (10%)
58	37857.2	264.2	0	H-11->L+2 (15%), H-7->L+2 (75%)
59	37941.1	263.6	0.0001	H-3->L+3 (91%)
60	37987.9	263.2	0.0001	HOMO->L+5 (10%), HOMO->L+8 (77%)

**Table S6** Electronic transitions calculated for **5a**

No.	Energy (cm <sup>-1</sup> )	Wavelength (nm)	Osc. Strength	Major contribs
1	18607.2	537.4	0.0583	HOMO->LUMO (36%), HOMO->L+1 (47%)
2	19129.1	522.8	0.0759	HOMO->LUMO (49%), HOMO->L+1 (34%)
3	19896.1	502.6	0	H-3->L+5 (47%), HOMO->L+5 (31%)
4	20263.9	493.5	0.0003	H-4->L+5 (88%)
5	20966.4	477.0	0	H-2->L+5 (77%)
6	22426.2	445.9	0.1697	H-3->LUMO (12%), H-1->LUMO (18%), H-1->L+1 (52%)
7	22811.8	438.4	0.0838	H-3->L+1 (14%), H-2->LUMO (41%), H-1->LUMO (24%), H-1->L+1 (11%)
8	23240.9	430.3	0.0004	H-4->LUMO (35%), H-4->L+1 (64%)
9	23410.2	427.2	0.0008	H-3->L+1 (10%), H-2->LUMO (31%), H-2->L+1 (51%)
10	23665.1	422.6	0	H-4->LUMO (64%), H-4->L+1 (35%)
11	23790.1	420.3	0.0946	H-3->LUMO (16%), H-3->L+1 (12%), H-2->LUMO (20%), H-2->L+1 (30%), H-1->LUMO (12%)
12	25510.5	392.0	0.5795	H-3->LUMO (48%), H-3->L+1 (21%), H-1->L+1 (11%)
13	26370.3	379.2	1.0566	H-3->LUMO (16%), H-3->L+1 (33%), H-1->LUMO (24%), HOMO->L+1 (10%)
14	26636.5	375.4	0.0063	H-18->L+5 (95%)
15	26645.3	375.3	0	H-6->LUMO (12%), H-5->LUMO (85%)
16	27001.8	370.3	0	H-6->L+1 (83%), H-5->L+1 (12%)
17	27999.5	357.1	0.0005	H-7->LUMO (97%)

18	28398.8	352.1	0.0004	H-8->L+1 (96%)
19	28556.1	350.2	0	H-9->LUMO (42%), H-9->L+1 (46%)
20	29598.1	337.9	0	H-6->L+1 (13%), H-5->L+1 (84%)
21	29719.9	336.5	0	H-6->LUMO (85%), H-5->LUMO (12%)
22	29853.0	335.0	0	HOMO->L+2 (97%)
23	30306.3	330.0	0	H-3->L+5 (22%), HOMO->L+5 (64%)
24	30357.9	329.4	0.0005	H-7->L+1 (96%)
25	30541.8	327.4	0.0125	H-10->LUMO (24%), H-8->LUMO (67%)
26	30568.4	327.1	0.0241	H-10->LUMO (50%), H-10->L+1 (12%), H-8->LUMO (30%)
27	30971.7	322.9	0.0145	H-10->LUMO (19%), H-10->L+1 (78%)
28	31022.5	322.3	0.0889	HOMO->L+3 (79%), HOMO->L+4 (11%)
29	31391.9	318.6	0	H-1->L+5 (88%)
30	31516.1	317.3	0	H-9->LUMO (55%), H-9->L+1 (43%)
31	31820.2	314.3	0.0568	HOMO->L+3 (15%), HOMO->L+4 (79%)
32	31835.5	314.1	0	H-1->L+2 (95%)
33	33334.9	300.0	0.0073	H-1->L+3 (97%)
34	33444.6	299.0	0	H-11->LUMO (72%), H-11->L+1 (27%)
35	34216.5	292.3	0.0442	H-12->LUMO (18%), H-12->L+1 (18%), H-1->L+4 (61%)
36	34336.6	291.2	0.0006	H-11->LUMO (27%), H-11->L+1 (72%)
37	35027.9	285.5	0.0301	H-12->LUMO (66%), H-1->L+4 (26%)
38	35090.0	285.0	0.1196	H-12->LUMO (11%), H-12->L+1 (75%)
39	35727.9	279.9	0	HOMO->L+6 (97%)
40	36040.1	277.5	0	H-2->L+2 (99%)
41	36094.9	277.0	0	HOMO->L+7 (96%)
42	36494.2	274.0	0	H-3->L+2 (98%)
43	36597.4	273.2	0.1284	H-13->LUMO (14%), H-2->L+3 (34%), H-2->L+4 (34%)
44	36795.8	271.8	0	H-18->LUMO (39%), H-18->L+1 (57%)
45	36899.1	271.0	0.0906	H-15->L+1 (16%), H-13->LUMO (16%), H-13->L+1 (32%)
46	37046.7	269.9	0.0004	H-4->L+3 (26%), H-4->L+4 (54%)
47	37304.8	268.1	0	H-18->LUMO (57%), H-18->L+1 (41%)
48	37338.6	267.8	0	H-4->L+2 (100%)
49	37350.7	267.7	0.0436	H-13->LUMO (42%), H-3->L+3 (25%), H-3->L+4 (11%)
50	37523.3	266.5	0.0008	H-3->L+3 (11%), H-2->L+3 (47%), H-2->L+4 (17%)
51	37657.2	265.6	0	H-9->L+3 (17%), H-9->L+4 (54%)

52	37704.8	265.2	0.0627	H-13->L+1 (16%), H-3->L+3 (24%), H-2->L+4 (30%)
53	37771.8	264.7	0.0026	HOMO->L+10 (80%)
54	37832.2	264.3	0.0214	H-16->LUMO (26%), H-16->L+1 (13%), H-15->LUMO (11%), H-15->L+1 (16%), H-13->L+1 (13%), HOMO->L+10 (13%)
55	37956.5	263.5	0.0012	HOMO->L+9 (93%)
56	38017.7	263.0	0.0375	H-16->LUMO (16%), H-15->LUMO (12%), H-3->L+3 (27%), H-3->L+4 (12%)
57	38289.6	261.2	0.0104	H-16->LUMO (16%), H-16->L+1 (11%), H-15->LUMO (14%), H-15->L+1 (24%), H-3->L+4 (21%)
58	38387.2	260.5	0.0118	H-15->LUMO (39%), H-3->L+4 (38%)
59	38506.5	259.7	0.0061	H-17->L+1 (26%), H-16->L+1 (33%), H-14->LUMO (10%), H-14->L+1 (15%)
60	38688.0	258.5	0	H-1->L+7 (88%)

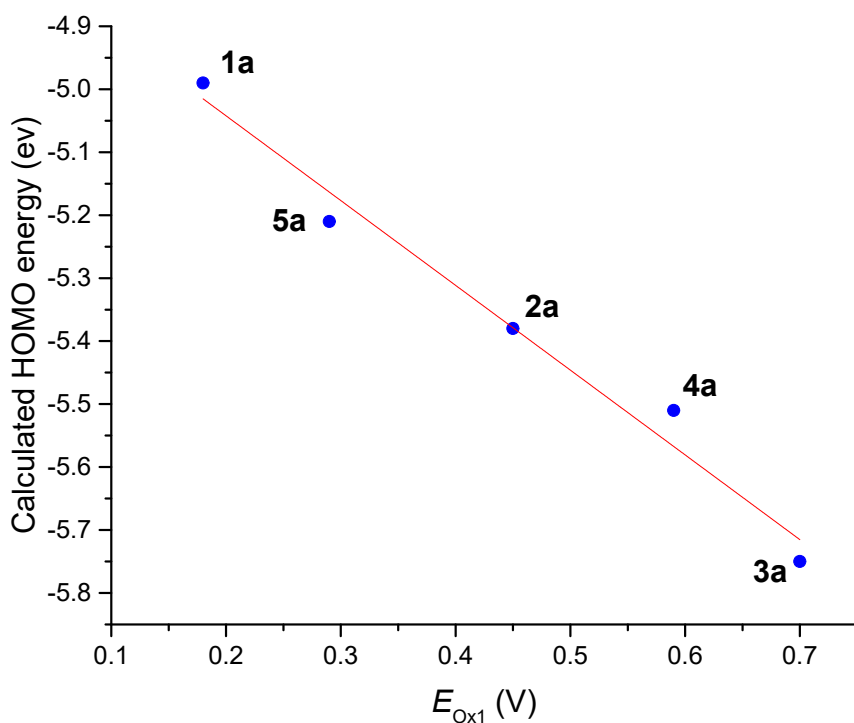


**Figure S56** Correlations of calculated HOMO energy with the first oxidation potentials for the compounds **1a-5a**.

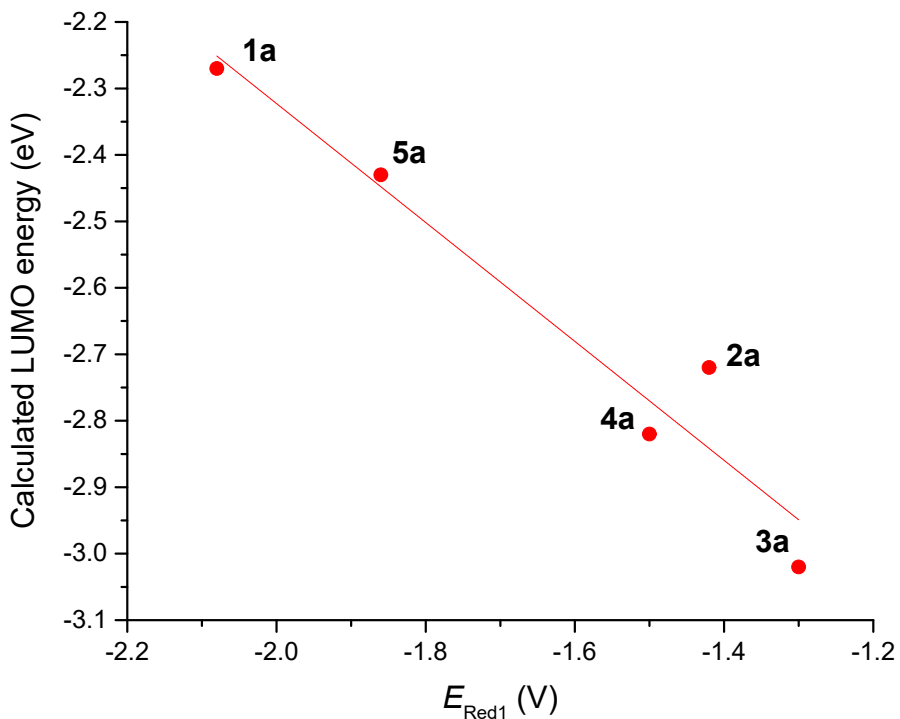


**Figure S57** Correlations of calculated LUMO energy with the first reduction potentials for the compounds **1a-5a**.

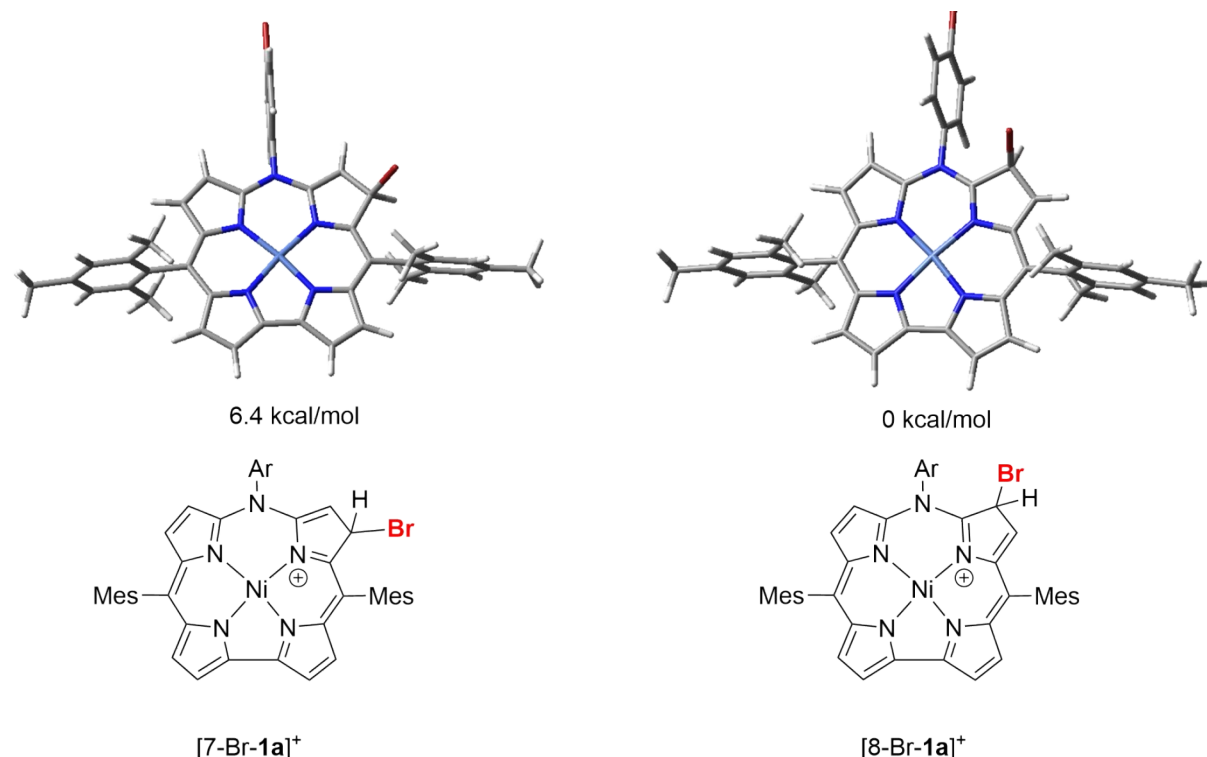


**Figure S58** DFT optimized models and relative energies of possible cationic intermediates that can be formed upon addition of one bromine atom in the C7 or C8 site.

**Table S7.** Computational details for the optimized structures of compounds using Gaussian<sup>1</sup> and NBO<sup>2</sup> software packages

Structure / Name <sup>[a]</sup>	SCF E	ZPV <sup>[b]</sup>	lowest freq.	E	ΔH	ΔG <sup>[c]</sup>	HOMO	LUMO	HLG
	a.u.	a.u.	cm <sup>-1</sup>	a.u.	a.u.	a.u.	eV	eV	eV
<b>1a</b> / Azacor-OF_a	-5975.541546	-5974.888266	7.24	-5974.845169	-5974.844224	-5974.971043	4.99	2.27	2.72
<b>2a</b> / AzacorNO2-OF_a	-6179.879760	-6179.223692	7.73	-6179.177988	-6179.177043	-6179.308791	5.36	2.72	2.64
<b>3a</b> / Azacor2NO2-OF_a	-6384.216142	-6383.557340	12.67	-6383.509010	-6383.508066	-6383.644684	5.74	3.02	2.72
<b>4a</b> /									
AzacorBr6-OF_a	-21415.096807	-21414.505078	7.05	-21414.452161	-21414.451217	-21414.604130	5.52	2.82	2.70
<b>5a</b> / AzacorAc-OF_a	-6128.075675	-6127.384978	12.98	-6127.338282	-6127.337338	-6127.471184	5.21	2.43	2.78
[8-Br- <b>1a</b> ] <sup>*</sup> / AzacorBr+-OF_a	-8549.179829	-8548.524711	13.73	-8548.479780	-8548.478836	-8548.609811	-	-	-
[7-Br- <b>1a</b> ] <sup>*</sup> / AzacorBr+-OF_a2	-8549.168509	-8548.514201	6.97	-8548.469181	-8548.468236	-8548.599608	-	-	-

[a] Data set name (Cartesian coordinates available as \*.pdb files). [b] Zero-point vibrational energy. [c] Gibbs free energy.

- [1] Gaussian 16, Revision C.01, Frisch, M. J.; Trucks, G. W.; Schlegel, H. B.; Scuseria, G. E.; Robb, M. A.; Cheeseman, J. R.; Scalmani, G.; Barone, V.; Petersson, G. A.; Nakatsuji, H.; Li, X.; Caricato, M.; Marenich, A. V.; Bloino, J.; Janesko, B. G.; Gomperts, R.; Mennucci, B.; Hratchian, H. P.; Ortiz, J. V.; Izmaylov, A. F.; Sonnenberg, J. L.; Williams-Young, D.; Ding, F.; Lipparini, F.; Egidi, F.; Goings, J.; Peng, B.; Petrone, A.; Henderson, T.; Ranasinghe, D.; Zakrzewski, V. G.; Gao, J.; Rega, N.; Zheng, G.; Liang, W.; Hada, M.; Ehara, M.; Toyota, K.; Fukuda, R.; Hasegawa, J.; Ishida, M.; Nakajima, T.; Honda, Y.; Kitao, O.; Nakai, H.; Vreven, T.; Throssell, K.; Montgomery, J. A., Jr.; Peralta, J. E.; Ogliaro, F.; Bearpark, M. J.; Heyd, J. J.; Brothers, E. N.; Kudin, K. N.; Staroverov, V. N.; Keith, T. A.; Kobayashi, R.; Normand, J.; Raghavachari, K.; Rendell, A. P.; Burant, J. C.; Iyengar, S. S.; Tomasi, J.; Cossi, M.; Millam, J. M.; Klene, M.; Adamo, C.; Cammi, R.; Ochterski, J. W.; Martin, R. L.; Morokuma, K.; Farkas, O.; Foresman, J. B.; Fox, D. J. Gaussian, Inc., Wallingford CT, 2016.
- [2] NBO Version 3.1, E. D. Glendening, A. E. Reed, J. E. Carpenter, and F. Weinhold